Long-wave instabilities of evaporating/condensing viscous film flowing down a wavy inclined wall: Interfacial phase change effect of uniform layers

Sanghasri Mukhopadhyay, Nicolas Cellier, Asim Mukhopadhyay

Long-wave instabilities of evaporating/condensing viscous film flowing down a wavy inclined wall: Interfacial phase change effect of uniform layers

Sanghasri Mukhopadhyay,[1] Nicolas Cellier,[2] and Asim Mukhopadhyay[3,a)]

AFFILIATIONS

[1]Department of Mathematics, IIT Madras, Chennai, India
[2]Department of Industrial Engineering, IMT Mines Albi, Toulouse University, 81013 Albi Cedex 9, France
[3]Department of Mathematics, Vivekananda Mahavidyalaya, Burdwan, West Bengal, India

ABSTRACT

The interfacial phase change effect on a thin film flowing down an undulated wall has been investigated in the present study. The study is performed for a general periodic undulated bottom of moderate steepness that is long compared to the film thickness, followed by a case study over the sinusoidal bottom. The long-wave instabilities of the ununiform film are used by deriving a nonlinear evolution equation in the classical long-wave expansion method framework. The one-equation model can track the free surface evolution and involve the bottom undulation, viscosity, gravity, surface tension, and phase change (evaporation/condensation) effects. Linear stability analysis shows that the bottom steepness ζ has a dual role. In the downhill region, increasing ζ destabilizes, whereas increasing ζ stabilizes in the uphill region. Weakly nonlinear waves are studied using the method of multiple scales to obtain the complex Ginzburg–Landau equation. The results show that both supercritical and subcritical solutions are possible for evaporating and condensate film. Interestingly, while one subcritical region is visible for an evaporating film, two subcritical unstable regions are found for condensate film. The numerical solution of the free-surface equation demonstrates the finite-amplitude behavior that tends to dry out for an evaporating film. For condensate film, the thickness increases rapidly. The rupture dynamics highly depend on the initial perturbation, and the bottom steepness has a negligible effect on it. Kutateladze number has a significant impact on the stability characteristic of the film flow as it represents a sort of efficiency of phase change that occurs at the interface.

I. INTRODUCTION

Falling liquid film on an inclined/vertical plane substrate is one of the most important hydrodynamic problems that exhibit a wide variety of spatial and temporal structures. It is a convectively unstable open-flow hydrodynamic system, governed by Navier–Stokes equations coupled with equation of continuity with appropriate boundary conditions, except when the Reynolds number and angle of inclination are small enough and surface tension is large enough and in that case flow remains parallel, laminar, and unidirectional down the plane surface. The problem is extensively studied experimentally, numerically, and analytically for a long time. Wave evolution on falling liquid film has been extensively studied over the last few decades, starting from the pioneering work by Kapitza and Kapitza.[1,2] Where a wide variety of wavy regimes, like a rolling wave with a capillary hill, a series of nearly solitary waves or almost harmonic waves of falling liquid films had been observed. In this situation, the stability and its criteria for falling films are needed to be understood. Reportedly, the beginning works in the field of stability analysis or falling films were done by Benjamin[3] and Yih[4] who investigated the long-wave instability of falling film over an inclined plane theoretically. They determined the phase velocity of the waves and critical Reynolds number for the transition, respectively. Benny[5] derived a wave evolution equation governing the flow by regular perturbation technique in terms of flow depth by expanding the variables in powers of the long-wave parameter. Turkyilmazoglu *et al.*[6,7] recently worked on the absolute and convective instabilities on boundary layer flow problems. An absolute instability is appropriate for unstable flow if its response to an impulse in time and space amplifies unboundedly everywhere in space for a large time.

A detailed review can be found previous research studies.[8–13]

In industrial chemistry, the liquid phase is generated in the form of a thin layer, and while moving, it comes in the interaction with the gas flow. Liquid particles in the layer are mixed up substantially, increasing inter-phasic heat and mass transfer. Films play the role of activating medium for heat transfer in drip and tower coolers, scrubbers and rectifying columns, steam boilers, evaporators, and oil-refining equipment.

In 1916, Nusselt first analytically investigated the laminar film condensation on a vertical plate. There are several improvements in Nusselt's analysis over the next few years, but until 1970 the stability analysis of film flow with phase change was never investigated. Sparrow *et al.*[14] investigated the problem of laminar-film condensation on a vertical plate by using boundary layer theory. They found a similarity transformation, which reduced the governing partial differential equation (PDE) to ordinary differential equation (ODE), and concluded that the effect of Prandtl number is significant for its small values ($Pr \ll 1$), that is, when the thermal boundary layer is larger than the momentum boundary layer, its effect is minimal for large Prandtl number ($Pr \gg 1$). Later, Bankoff,[15] Marschall and Lee,[16] and Lin[17] successively reported the stability of condensate film flow down a vertical/inclined plane. Ünsal and Thomas[18] presented a linear stability analysis for condensate film flow considering the effect of mass transfer at the interface due to phase change. Subsequently, Ünsal and Thomas[19] also published another work addressing the nonlinear stability of vertical condensate film flow by using the perturbation method. Spindler[20] studied the linear stability of liquid films with interfacial phase change in a more detailed form and reported that evaporation has a destabilizing influence while condensation a stabilizing one. Kocamustafaogullari[21] investigated two-fluid model formulations in analyzing the interfacial stability of liquid film flows. The author claimed that the interfacial stability analysis developed within the two-fluid model formulation frame is quite accurate as judged by comparing its results with the available experimental data. Hwang and Weng[22] studied finite-amplitude stability analysis of liquid films down a vertical flat wall with and without interfacial phase change. By considering a generalized kinematic equation for the film thickness, the authors investigated by the method of perturbation. They showed that mass transfer into (away from) the liquid phase would stabilize (destabilize) the film flow. Joo *et al.*[23] investigated the long-wave instability of volatile viscous falling film draining down a uniformly heated inclined plane by deriving an evolution equation for the two-dimensional disturbances considering the effects of thermocapillary and evaporation and determines the propensity for dry out of the film. Gambaryan-Roisman[24] studied the influence of non-uniformity of substrate thermal conductivity on the hydrodynamics and heat transfer in thin liquid films accounting for the effects of surface tension, thermocapillary, and evaporation. Recently, Abderrahmane[25] investigated the stability of evaporating (condensing) liquid film flowing down an inclined plane using the energy integral method. The author showed that evaporation (condensation) destabilizes (stabilizes) the film flow.

The above studies are focused only on the film flow down flat inclined/vertical substrates, but in most applications, the film does not flow over a perfectly flat substrate. During the last few decades, many advancements have been made in renewable energy, for example, solar energy, wind energy, and waste heat from industrial wastages. Solar energy is used in solar refrigeration, solar heat storage, or transportation of heat or cooling over a large distance. The process of absorption/desorption is widely used. In most cases, the apparatus is built purposefully with the wavy surface, while in other applications, the corrugation is unavoidable. Thus, in either case, it is of our interest to investigate how the alterations from the ideal condition of a flat inclined affect the gravity-driven film flow with various physical effects. The hydrodynamics of falling liquid film down an undulated surface has gained much attentiveness starting from the work of Pozrikidis[26] who have studied the free surface Stokes flow along with a sinusoidal topography. Later, Wierschem *et al.*[27] studied experimentally the linear stability of the film flow over modulations of moderate steepness that is long compared to the film thickness. They found that the critical Reynolds number for the onset of surface waves is higher than that for the flat bottom. Investigation of the viscous film flowing down a harmonic vertical substrate is done by Trifonov.[28,29] The author has contemplated the effect of surface tension, viscosity, and inertia. Tougou[30] investigated theoretically the influence of a weakly wavy bottom on the stability of steady film flow. Mogilevskiy and Shkadov[31] have used the integral boundary layer approach to model the problem of a thin film flow on a weakly wavy wall. They showed the topography can both stabilize and destabilize the flow, depending on the corrugation period and the plane inclination angle. Veremieiev and Wacks[32] have developed the extension of the weighted residual model proposed by Ruyer-Quil and Manneville[33] and D'Alessio *et al.*[34] and included the third and fourth terms in the long-wavelength expansion to enlarge a new modeling strategy for flow on an inclined corrugated substrate. Other researchers, like Trifonov,[35] Vlachogiannis and Bontozoglou,[36] Wierschem and Aksel,[37] Wierschem *et al.*,[38,39] Dávalos-Orozco,[40,41] Häcker and Uecker,[42] Heining and Aksel,[43,44] Heining *et al.*,[45] etc., have also studied the effect of bottom topography in the flow of falling films for several physical problems. An excellent review about the film flow on different topography can be found in a piece of work by Aksel and Schörner.[46]

This study shall present the analysis of finite-amplitude long-wave instability to characterize evaporating (condensate) viscous thin film flowing over inclined wavy bottom incorporating phase change effect at the interface. It is expected that the undulated bottom topography may have a significant impact on the stability characteristic of the evolution of a non-isothermal film flow undergoing a phase change (evaporation/condensation) at the interface.

To the best of our knowledge, the study of the hydrodynamics of falling viscous film through an undulated surface with a phase change effect has not been studied intensively so far. Our study will help to explore a broader gateway to handle many industrial and natural phenomena.

II. FORMULATION OF THE PROBLEM

Let us consider a thin viscous liquid film of density ρ, dynamic viscosity μ, thermal conductivity k_T, and surface tension σ flowing down an inclined wavy bottom $\hat{b}$. The fluid is assumed to be Newtonian with constant material properties. When the wavy bottom surface is heated (cooled) at a fixed constant temperature T_w, which is higher (lower) than the saturation temperature T_s of the fluid, the evaporation (condensation) occurs at the liquid–vapor interface. The layer is evaporating (condensing) so that at the vapor–liquid interface, there is a mass loss (gain), momentum transfer, and energy consumption (deportation) that can affect the stability of the film flow.[47] The

liquid layer is bounded above by its vapor with density ρ^v, and as the layer is evaporating (condensing), the free surface is unbounded. The orthogonal Cartesian coordinates system identified by the orthonormal basis $\{e_{\hat{x}}, e_{\hat{y}}\}$ with O as origin is inclined at an angle β with respect to the horizontal, and the bottom profile $\hat{b}(\hat{x})$ is periodic with wavelength $\hat{\lambda}$ and amplitude $\hat{a}$, where $\hat{x}$ is in the direction of the main flow. It is useful and appropriate for an undulated bottom profile to introduce a local curvilinear coordinate system since the Nusselt solution is no longer a stationary solution. For the flow of thin films that are thinner than the radius of curvature of the bottom, the flow (u, v) is still mainly parallel to the bottom (see Fig. 1). Thus, at every point of the bottom $\hat{x}e_{\hat{x}} + \hat{b}(\hat{x})e_{\hat{y}}$, a local coordinate system identified by the orthonormal basis $\{e_x, e_y\}$ with e_x tangential and e_y normal to the bottom is defined. Thus, for an arbitrary point P within the fluid, the arc length x of the bottom and the distance y along e_y to the bottom are now taken as curvilinear coordinates. So in $e_{\hat{x}}$, $e_{\hat{y}}$ coordinates P $(\hat{x} - \sin\theta y, \hat{b}(\hat{x}) + \cos\theta y)$, where $\theta = \theta(\hat{x}) = \arctan(\partial\hat{b}(\hat{x})/\partial\hat{x})$ is the local inclination angle between $e_{\hat{x}}$ and e_x. This relation is always unique as we considered the film flow over the undulated bottom of moderate steepness that is long compared to the film thickness. To transform gradients, we will also need the bottom curvature κ, which is defined by

$$\kappa(\hat{x}) = -\frac{\partial^2\hat{b}(\hat{x})}{\partial\hat{x}^2}\left[1 + \left(\frac{\partial\hat{b}(\hat{x})}{\partial\hat{x}}\right)^2\right]^{-3/2}. \tag{1}$$

A. Governing equation

The flow field is characterized by balance in mass and momentum, described by the continuity equation and the Navier–Stokes equations, whereas the temperature field is governed by the equation of energy as follows:

$$\nabla\cdot\mathbf{V} = 0, \tag{2}$$

$$\rho\left(\frac{\partial\mathbf{V}}{\partial t} + (\nabla\cdot\mathbf{V})\mathbf{V}\right) = -\nabla p + (\rho - \rho^v)g + \mu\nabla^2\mathbf{V}, \tag{3}$$

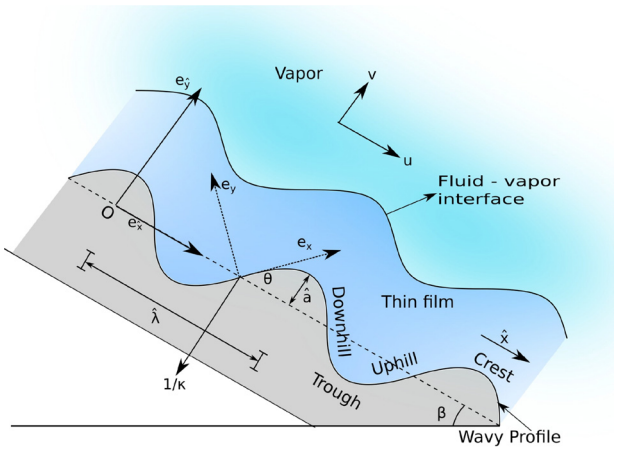

FIG. 1. Diagrammatic picture.

$$\frac{\partial T}{\partial t} + (\mathbf{V}\cdot\nabla)T = k_c\nabla^2 T, \tag{4}$$

where $\nabla = \frac{1}{1+\kappa y}\mathbf{e}_x\frac{\partial}{\partial x} + \mathbf{e}_y\frac{\partial}{\partial y}$, $\mathbf{V} = u\,\mathbf{e}_x + v\,\mathbf{e}_y$ is the liquid velocity, g is the acceleration due to gravity, and k_c is the thermal diffusivity of the liquid. For detailed derivation of the governing equations, we refer the reader to the studies by Wierschem *et al.*[27] and Mukhopadhyay and Mukhopadhyay.[48]

The boundary conditions at the wavy bottom $y = 0$ are the usual no-slip condition of velocity and a constant wall temperature,

$$\mathbf{V} = 0, \quad T = T_w. \tag{5}$$

The boundary conditions at the fluid–vapor interface $y = h(x, t)$ are the balance of tangential and normal stresses, the relation of interfacial energy balances, and the equality of fluid and saturated vapor temperatures:[18,49] the tangential and normal stress balances are taken as follows:

$$\mathbf{n}\cdot\boldsymbol{\tau}\cdot\mathbf{t} = 0, \tag{6}$$

$$p^v + \mathbf{n}\cdot\boldsymbol{\tau}\cdot\mathbf{n} - \frac{\gamma - 1}{\rho\gamma}\left(-\frac{k_T}{h_{fg}}(\nabla T).\mathbf{n}\right)^2 = -\sigma\nabla\cdot\mathbf{n}, \tag{7}$$

$$k_T(\nabla T)\cdot\mathbf{n} - \rho h_{fg}[h_t + \mathbf{V}\cdot\nabla(h - y)] = 0, \tag{8}$$

$$T = T_s, \tag{9}$$

where p^v, h_{fg}, and $\gamma = \rho^v/\rho$ are the vapor pressure, latent heat of phase change, and ratio of vapor density to liquid density, respectively, and

$$\mathbf{n} = \frac{\mathbf{e}_y - \frac{1}{1+\kappa h}h_x\mathbf{e}_x}{\sqrt{1 + \left(\frac{1}{1+\kappa h}h_x\right)^2}}, \quad \mathbf{t} = \frac{\mathbf{e}_x + \frac{1}{1+\kappa h}h_x\mathbf{e}_y}{\sqrt{1 + \left(\frac{1}{1+\kappa h}h_x\right)^2}}, \tag{10}$$

are the unit normal and tangential vector, respectively. For detailed derivation of boundary conditions, we refer the reader to the studies by Ünsal and Thomas,[50] Joo *et al.*,[23] and Mukhopadhyay and Mukhopadhyay.[51]

The basic velocity $[u(y), 0]$ in the steady flow down the inclined flat bottom $\kappa = 0$ is

$$U = \frac{3}{2}\langle u\rangle\left[1 - \left(1 - \frac{y}{\hat{h}}\right)^2\right]. \tag{11}$$

To obtain Eq. (11), the no-slip at the bottom $u(0) = 0$ and zero shear stress at the free surface $\frac{\partial u}{\partial y}|_h = 0$ are used. Here, $\langle u\rangle$ is the depth averaged velocity and $\hat{h}$ is the averaged thickness of the film, where $\langle u\rangle = (1 - \gamma)g\sin\beta\hat{h}^2/3\nu$ is the averaged basic velocity.

B. Scaling and non-dimensionalization

Before solving, we rewrite the problem precisely in dimensionless format. The dimensionless quantities are defined as follows:

$$x^* = \frac{2\pi}{\hat{\lambda}}x, \quad y^* = \frac{1}{\hat{h}}y, \quad h^* = \frac{1}{\hat{h}}h, \quad u^* = \frac{1}{\langle u\rangle}u,$$
$$v^* = \frac{\hat{\lambda}}{2\pi\hat{h}\langle u\rangle}v, \quad t^* = \frac{2\pi\langle u\rangle}{\hat{\lambda}}t, \quad \kappa^* = \frac{\hat{\lambda}^2}{4\pi^2\hat{a}}\kappa,$$
$$p^* = \frac{1}{\rho\langle u\rangle^2}p, \quad T^* = \frac{T-T_w}{T_s-T_w}, \quad \hat{x}^*(x^*) = \frac{2\pi}{\hat{\lambda}}\hat{x}(x), \tag{12}$$
$$\hat{b}^*(\hat{x}^*) = \frac{1}{\hat{a}}\hat{b}\left(\frac{\hat{\lambda}}{2\pi}\hat{x}^*\right), \quad \theta^* = \arctan\left(\zeta\frac{\partial\hat{b}^*}{\partial\hat{x}^*}\right),$$

where $\zeta = 2\pi\hat{a}/\hat{\lambda}$ is the bottom steepness and $\varepsilon = 2\pi\hat{h}/\hat{\lambda}$ is the aspect ratio. Yet, it is noteworthy that to study the effect of bottom undulation on the flow, the thin film flow over a flat bottom as a reference is used. Thus, the average velocity of the mean flow over flat film, $\langle u\rangle$, and the constant film thickness, $\hat{h}$, are taken as the characteristic velocity and length scale along the normal direction of the mean flow, respectively, whereas $\hat{\lambda}$ is the characteristic longitudinal length scale whose order may be considered the same as the wavelength of the free surface wave, which is very long compared to the film thickness.

Using the dimensionless quantities (12) in the governing equations (2)–(9)

$$\frac{1}{1+\varepsilon\zeta\kappa y}\left(\frac{\partial u}{\partial x}+\varepsilon\zeta\kappa v\right)+\frac{\partial v}{\partial y}=0, \tag{13}$$

$$\varepsilon Re\left(\frac{\partial u}{\partial t}+u\frac{\partial u}{\partial x}+v\frac{\partial u}{\partial y}\right)=-\varepsilon Re\frac{\partial p}{\partial x}+3SS+\frac{\partial^2 u}{\partial y^2}+\varepsilon\kappa\zeta\frac{\partial u}{\partial y}+O(\varepsilon^2), \tag{14}$$

$$-\varepsilon Re\zeta\kappa u^2=-Re\frac{\partial p}{\partial y}-3CS+\varepsilon\frac{\partial^2 v}{\partial y^2}+O(\varepsilon^2), \tag{15}$$

$$\varepsilon RePr\left(\frac{\partial T}{\partial t}+u\frac{\partial T}{\partial x}+v\frac{\partial T}{\partial y}\right)=\frac{\partial^2 T}{\partial y^2}+\varepsilon\zeta\kappa\frac{\partial T}{\partial y}+O(\varepsilon^2), \tag{16}$$

where $SS=\frac{\sin(\beta-\theta)}{\sin\beta}$ and $CS=\frac{\cos(\beta-\theta)}{\sin\beta}$

$$u=0, \quad v=0, \quad \text{and} \quad T=0. \tag{17}$$

At the free surface $y=h(x,t)$,

$$\frac{\partial u}{\partial y}+\varepsilon\left(2\zeta\kappa h\frac{\partial u}{\partial y}-\zeta\kappa u\right)+O(\varepsilon^2)=0, \tag{18}$$

$$p_a-p+\frac{2\varepsilon}{Re}\left(\frac{\partial v}{\partial y}+\frac{\partial u}{\partial y}h_x\right)+(\gamma-1)NdRe^{-2}\left(\frac{\partial T}{\partial y}\right)^2 = \varepsilon^2 We(h_{xx}-\zeta\varepsilon^{-1}\kappa+2\zeta^2\kappa^2 h), \tag{19}$$

$$\frac{Ku}{\varepsilon Pe}\left(\frac{\partial T}{\partial y}-\varepsilon^2 h_x\frac{\partial T}{\partial x}\right)=h_t+uh_x-v-\varepsilon\zeta\kappa hu\frac{\partial h}{\partial x}+O(\varepsilon^2), \tag{20}$$

$$T=1, \tag{21}$$

where $Re(\equiv\langle u\rangle\hat{h}/\nu)$ is the Reynolds number, $We(\equiv\sigma/\rho\langle u\rangle^2\hat{h})$ is the Weber number, $Pr(\equiv\nu/k_c)$ is the Prandtl number, and $Pe=RePr$ is the Péclet number. $Ku(\equiv C_p(T_s-T_w)/h_{fg})$ is the Kutateladze number, which is reciprocal of Jacob number. Ku accounts the effect of the phase change. $Ku>0$ corresponds to the condensate film, $Ku<0$ to the evaporating film flow, and $Ku=0$ corresponds to the isothermal film. $Nd(\equiv Ku^2/\gamma Pr^2)$ is the vapor recoil number. The effect of Nd has been found to be negligible on stability,[18] so Nd/Re^2 is assumed as $O(\varepsilon^2)$.[49] That is, the effect of vapor recoil is assumed to be negligible.[24]

III. LONG-WAVE APPROXIMATION AND CONSTRUCTION OF MODEL

We are now interested in yielding a nonlinear evolution equation in terms of non-dimensional film thickness $h(x, t)$, depending on the dimensionless spatial and temporal variables x and t.

Since the long-wavelength modes are the most unstable ones for film flow, expanding the physical quantities u, v, p, and T as a power series,

$$u=u_0+\varepsilon u_1+\cdots, \quad v=v_0+\varepsilon v_1+\cdots,$$
$$p=p_0+\varepsilon p_1+\cdots, \quad T=T_0+\varepsilon T_1+\cdots \tag{22}$$

and substituting the above into the governing equations (13)–(16) and the boundary conditions (17)–(21) and then collecting the coefficients of like powers of ε and solving up to $O(\varepsilon)$ (for details see Appendix A and Mukhopadhyay and Mukhopadhyay[48,52])

$$\bar{u}_0=SSh^2, \tag{23}$$

$$T_0=\frac{y}{h}, \tag{24}$$

$$\bar{u}_1=\frac{6}{5}h^5 ReSS^2 h_x-\frac{5}{8}\frac{Ku}{\varepsilon Pr}SSh^2+\frac{1}{3}\varepsilon^2 ReWe \times\left[4h\zeta^2\kappa\kappa_x+h_{xxx}+\varepsilon^{-1}\zeta\kappa_x+2\zeta^2\kappa^2 h_x\right] -h^2 CSh_x+\frac{9}{8}h^3 SS\zeta\kappa, \tag{25}$$

$$T_1=\left(\frac{1}{6}\frac{Ku}{\varepsilon h}-\frac{1}{5}RePrSSh^2h_x+\frac{1}{2}\zeta\kappa\right)y-\frac{1}{4}\zeta\kappa y^2 \times\left(-\frac{1}{6}\frac{Ku}{\varepsilon h^3}+\frac{1}{2}RePrSSh_x\right)y^3-\frac{3}{8}\frac{RePrSS}{h}h_x y^4 +\frac{3}{40}\frac{RePrSS}{h^2}h_x y^5, \tag{26}$$

where $\bar{u}_{0,1}=(1/h)\int_0^h u_{0,1}dy$.

Integrating the continuity equation (13) with respect to y from 0 to h by using Leibniz's rule and boundary conditions (17) and (20), we have

$$h_t-\frac{Ku}{\varepsilon Pe}\left[(T_{0z}+\varepsilon T_{1z})-\varepsilon^2(T_{0x}+\varepsilon T_{1x})h_x\right] +\frac{\partial}{\partial x}\left[(\bar{u}_0+\varepsilon\bar{u}_1)h\right]+O(\varepsilon^2)=0. \tag{27}$$

Substituting the values of T_0, T_1, $\bar{u}_0$, and $\bar{u}_1$ in Eq. (27), we get

$$h_t+P(h)+A(h)h_x+\varepsilon(B(h)h_{xx}+\varepsilon^2 C(h)h_{xxxx}) +D(h)h_x^2+E(h)h_xh_{xxx}+O(\varepsilon^2)=0, \tag{28}$$

where

$$P(h)=-\frac{Ku}{\varepsilon Pe}\left[\left(1-\frac{Ku}{3}\right)\frac{1}{h}-\frac{1}{2}\varepsilon\zeta\kappa\right], \tag{29}$$

$$A(h)=\left(3SS-\frac{7}{40}KuSS-\frac{15}{8}\frac{Ku}{Pr}SS\right)h^2 +\varepsilon\left[\frac{3}{2}SS\zeta\kappa h^3+\varepsilon^2 WeRe\left(-\zeta\varepsilon^{-1}+\frac{8}{3}\kappa h\zeta^2\right)h^2\frac{\partial\kappa}{\partial x}\right], \tag{30}$$

$$B(h) = \frac{6}{5} ReSS^2 h^6 - CSh^3 + \frac{1}{3}\varepsilon^2 WeRe\zeta^2\kappa^2 h^3, \tag{31}$$

$$C(h) = \frac{1}{3} WeReh^3, \tag{32}$$

$$D(h) = \varepsilon^2 P(h) + B'(h), \tag{33}$$

$$E(h) = C'(h). \tag{34}$$

Here, prime ($'$) denotes the derivatives of respective quantities with respect to h.

IV. CASE STUDY

Our aim for this work is to present the entire study for a general undulated bottom profile $\hat{b}$. Also, we intend to discuss the results for a particular case study by choosing a sinusoidal bottom profile as follows:

$$\hat{b}(\hat{x}) = \hat{a}\cos(2\pi\hat{x}/\hat{\lambda}), \tag{35}$$

where $\hat{\lambda}$ is the wavelength and $\hat{a}$ is the amplitude of the wavy bottom profile. The downhill portion is $0 < \hat{x} < \hat{\lambda}/2$ and the uphill portion is $\hat{\lambda}/2 < \hat{x} < \hat{\lambda}$. $\hat{x} = 0$ is the crest and $\hat{x} = \hat{\lambda}/2$ is the trough. For graphical understanding, we refer to Fig. 1.

V. STABILITY ANALYSIS

Following Hwang and Weng[22] and Uma and Usha,[53] the non-dimensional film thickness for the perturbed state may be expanded in the following form:

$$h = 1 + \eta, \tag{36}$$

where η is the perturbation of the thickness.[18]

Substituting (36) in (28) and keeping the terms up to $O(\eta^3)$ and taking a transformation $x \to \varepsilon x$, $t \to \varepsilon t$, the evolution equation for perturbed state is found as follows:

$$\begin{aligned}
&\eta_t + P_1'\eta + A_1\eta_x + (B_1\eta_{xx} + C_1\eta_{xxxx}) \\
&\quad\times \frac{1}{2}P_1''\eta^2 + \frac{1}{6}P_1'''\eta^3 + \left(A_1'\eta + \frac{1}{2}A_1''\eta^2\right)\eta_x \\
&\quad\times \left(B_1'\eta + \frac{1}{2}B_1''\eta^2\right)\eta_{xx} + \left(C_1'\eta + \frac{1}{2}C_1''\eta^2\right)\eta_{xxxx} \\
&\quad\times (D_1 + D_1'\eta)\eta_x^2 + (E_1 + E_1'\eta)\eta_x\eta_{xxx} + O(\eta^4) = 0,
\end{aligned} \tag{37}$$

where P_1, A_1, B_1, C_1, and their corresponding derivatives with respect to h, which are denoted by primes, are evaluated at $h = 1$ from (29)–(32). The above transformation of coordinates is taken as the relatively slow spatial and temporal variations of the film thickness $h(x, t)$ justify lubrication-type approximation; as a consequence, it scales back to the original non-dimensional coordinates (x, y, t).[54]

It is worth mentioning that Eq. (37) of the disturbance $\eta(x, t)$ is obtained (i) by neglecting the derivatives of the averaged film thickness with respect to x in the unsteady equation, which corresponds to parallel flow approximation and (ii) by letting $\tilde{h} = 1$ in the unsteady

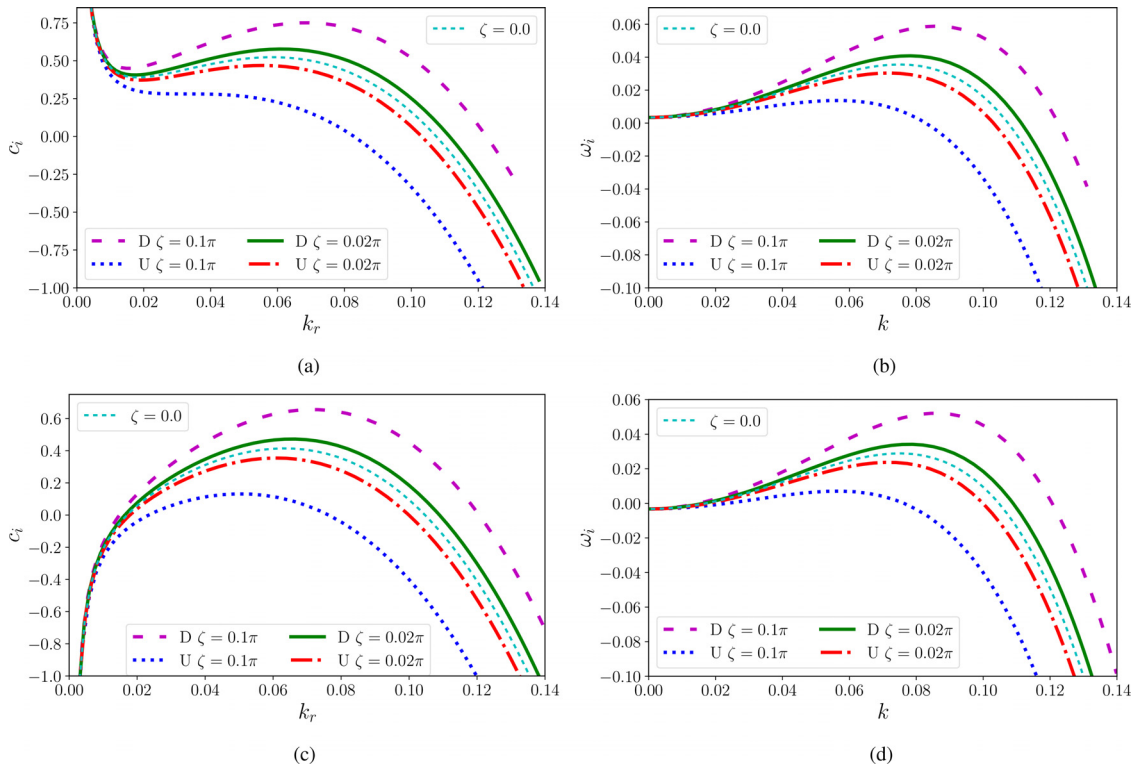

FIG. 2. Linear temporal growth rate curve (a) and (b) for evaporating film and (c) and (d) for condensate film at a point on the downhill (D, $\hat{x} = 1.57$) and point on the uphill (U, $\hat{x} = 4.71$) region for different bottom steepness ζ, when $Re = 10$, $Pr = 2.62$, and $Ka = 14\,133$. $\zeta = 0$ corresponds to a flat bottom. (a) For $Ku = -0.0872$, (b) for $Ku = -0.0872$, (c) for $Ku = 0.0872$, and (d) for $Ku = 0.0872$.

equation, which implies that the simplified unsteady equation is only locally valid.[22,53]

A. Linear stability analysis

To study the linear response for a sinusoidal perturbation of the film by assuming the perturbation of the form

$$\eta(x,t) = \Gamma \exp\left[i(kx - \omega t)\right] + c.c,$$

where Γ is the amplitude of the disturbance and *c.c* represents complex conjugate with real wave number k and complex frequency $\omega = \omega_r + i\,\omega_i$ of the linearized part of (37), we get the dispersion relation as follows:

$$Disp(\omega, k) \equiv -i\,\omega + i\,A_1 k + P_1' + (-B_1 k^2 + C_1 k^4) = 0. \tag{38}$$

Equating the real and the imaginary parts of (38), we get

$$\omega_r = A_1 k \quad \text{and} \quad \omega_i = -P_1' + (B_1 k^2 - C_1 k^4). \tag{39}$$

So, the linear phase velocity is

$$c_r = \frac{\omega_r}{k} = A_1, \tag{40}$$

which is non-dispersive in nature so that the group velocity of the perturbation equals to the phase velocity. The imaginary part of c is given by

$$c_i = \frac{\omega_i}{k} = -\frac{P_1'}{k} + (B_1 k - C_1 k^3). \tag{41}$$

The flow will be linearly stable, neutral, or unstable if $\omega_i <, =$ or > 0 respectively.

$\omega_i = 0$ implies

$$k^4\left(\frac{Ka\,Re^{1/3}}{3}\right) - k^2\left[\frac{6}{5}Re^2 SS^2 - CSRe + \varepsilon^2\left(\frac{Ka\,Re^{1/3}}{3}\right)\zeta^2\kappa^2\right] + \frac{Ku}{Pr}\left(1 - \frac{Ku}{3}\right) = 0, \tag{42}$$

where $Ka = Fi^{i/3} = \left(\frac{3\sigma^3}{\rho^3 g \nu^4 (1-\gamma)\sin\beta}\right)^{1/3}$ is the Kapitza number.

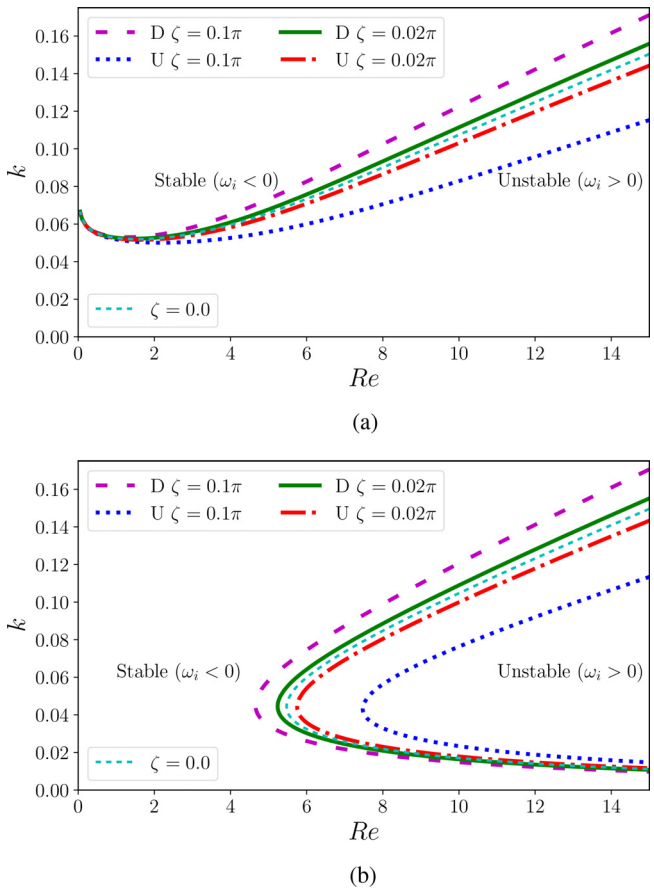

FIG. 3. Marginal stability curve (a) for evaporating film and (b) for condensate film; at a point on the downhill (D, $\hat{x} = 1.57$) and at a point on the uphill (U, $\hat{x} = 4.71$) region for different bottom steepness ζ, when $Pr = 2.62$ and $Ka = 14\,133$. $\zeta = 0$ corresponds to a flat bottom: (a) for $Ku = -0.0872$ and (b) for $Ku = 0.0872$.

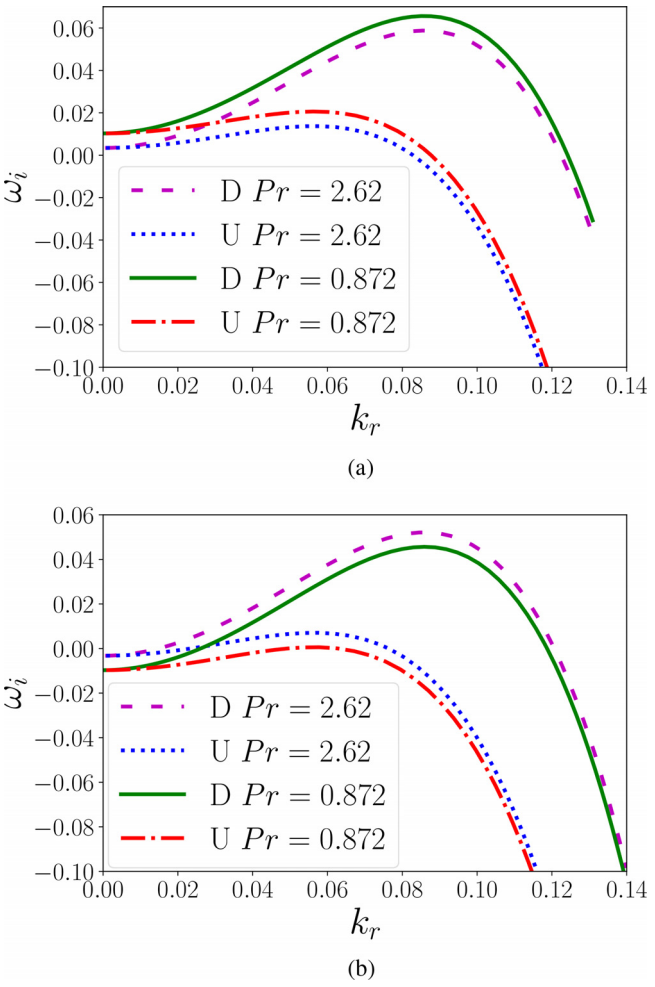

FIG. 4. Linear temporal growth rate curve for (a) evaporating film and (b) condensate film at a point on the downhill (D, $\hat{x} = 1.57$) and at a point on the uphill (U, $\hat{x} = 4.71$) region for $\zeta = 0.1\pi$, and different Pr values, when $Re = 10$ and $Ka = 14\,133$. (a) For $Ku = -0.0872$ and (b) for $Ku = 0.0872$.

For critical Re, we have

$$\frac{6}{5}Re^{11/6}SS^2 - CS\,Re^{5/6} + \left(\frac{\varepsilon^2 Ka\zeta^2\kappa^2}{3}\right)Re^{1/6} = \sqrt{\frac{4}{3}\frac{KaKu}{Pr}\left(1-\frac{Ku}{3}\right)}, \tag{43}$$

which is in good agreement with the results of Hwang and Weng[22] [Eq. (42) of their work] for vertical falling films on a flat plate. Again for $\zeta = 0$ and $Ku = 0$, we retrieve our standard result $Re_c = \frac{5}{6}\cot\beta$.[3,4]

1. Results from the case study

The dispersion relation (38) is solved using numerical continuation method[55] for a range of k values initiated from $k = 0$. The mesh is allowed to automatically adapt to the solution to equidistribute the local discretization error.[56] From Ref. 40, we see that the kind of wave we have for our case is non-dispersive, i.e., all waves of any wavenumber propagate at the same speed and arbitrary disturbances propagate without change of shape. The nature of the waves in the sense of stability is defined by the sign of the imaginary part of ω_i (or c_i). One interesting fact one can notice from this equation is $k \to 0$ implies $c_i \to \mp\infty$ depending on the sign upon the parameter Ku, that is what we can see from Figs. 2(a) and 2(c). Again from Eq. (39), $\omega_i \to -P_1'$ as $k \to 0$. This result is confirmed by Figs. 2(b) and 2(d). For both evaporating and condensing films, the linear growth rate in the uphill direction is smaller than the downhill direction, which is true for any moderately small steepness. Now, focusing on the marginal stability curves shown in Fig. 3, which separates k–Re plane into two regions, $\omega_i < 0$ gives a linear stable region as the perturbed small disturbance decays with the time and $\omega_i > 0$ gives linear unstable region as the perturbed small disturbance grows with the time. In both cases of evaporation [Fig. 3(a)] and condensation [Fig. 3(b)], the stable region increases for the flow in uphill region for a fixed value of ζ. One interesting fact is for downhill region, increasing ζ destabilizes and for uphill region increasing ζ stabilizes, i.e., ζ plays a dual role on stability. It is also very interesting to observe that, for condensing film, the critical Reynolds number (Re_c), the minimum Re in which instability sets in, increases in the uphill region than that of in the downhill region for a fixed bottom steepness parameter ζ but for evaporating film, it is always zero confirming that evaporating film is always unstable.

Another interesting fact is that an increase in Prandtl number plays a dual role in linear stability. From Fig. 4, it is clear that for an evaporating film ($Ku < 0$), increasing Pr stabilizes the flow and for condensate film ($Ku > 0$) destabilizes the flow, i.e., if we consider the evaporating film, for instance, when heat diffuses quickly in comparison with velocity, the linear growth rate of the perturbation increases. Also, these results are valid for both the uphill and downhill regions. This result is consistent with the previous works[18,22] for analysis over flat plates.

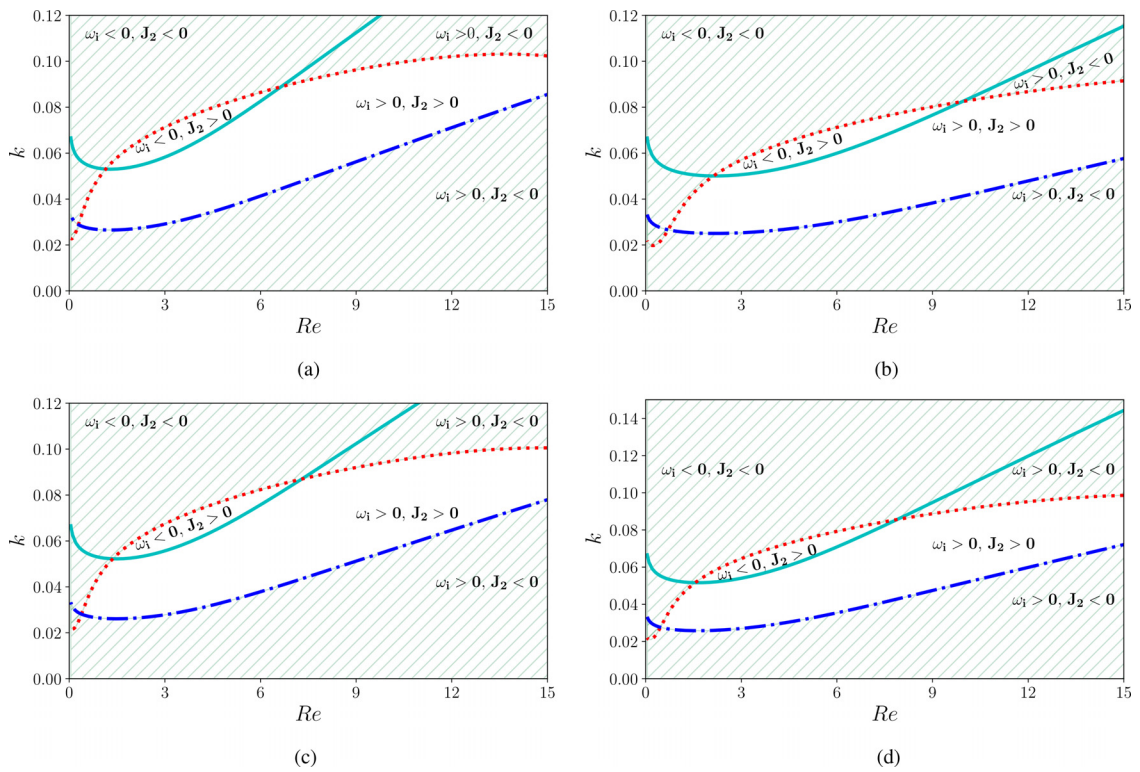

FIG. 5. Neutral stability curves for evaporating film for (a) $\zeta = 0.1\pi$, downhill, (b) $\zeta = 0.1\pi$, uphill, (c) $\zeta = 0.02\pi$, downhill, and (d) $\zeta = 0.02\pi$, uphill. Curves are plotted for $Pr = 2.62$ and $Ka = 14\,133$, $Ku = -0.0872$, and for various values of bottom steepness ζ in downhill ($\hat{x} = 1.57$) and uphill ($\hat{x} = 4.71$). (a) $\zeta = 0.1\pi$, downhill; (b) $\zeta = 0.1\pi$, uphill; (c) $\zeta = 0.02\pi$, downhill; and (d) $\zeta = 0.02\pi$, uphill.

B. Weakly nonlinear analysis

The linear stability analysis provides only first-hand information about the stability mechanism. Since the linear stability analysis is just a peek into the richness of the dynamics of unstable systems when finite amplitude effects are considered, to investigate the nonlinear effects on the stability threshold, a weakly nonlinear study is performed in this section.

Following Lin and Krishna,[57] it is almost a routine verification that Eq. (37) governing the flow can be asymptotically reduce to a complex Ginzburg–Landau equation in the vicinity of the criticality. For, introducing stretch time scales $t_1 = \alpha t$ and $t_2 = \alpha^2 t$ and long length scale $x_1 = \alpha x$ (α is the weakness of nonlinearity), so that the temporal and spatial derivatives become

$$\partial_t \to \partial_t + \alpha\partial_{t_1} + \alpha^2\partial_{t_2} \quad \text{and} \quad \partial_x \to \partial_x + \alpha\partial_{x_1}.$$

We have also taken the asymptotic expression $\eta = \alpha\eta_1 + \alpha^2\eta_2 + \alpha^2\eta_3 + \cdots$. Then, Eq. (37) yields

$$\begin{aligned}(L_0 + \alpha L_1 + \alpha^2 L_2 + \cdots)(\alpha\eta_1 + \alpha^2\eta_2 + \alpha^3\eta_3 + \cdots)\\ = -\alpha^2 N_2 - \alpha^3 N_3 + \cdots.\end{aligned} \tag{44}$$

The solution of Eq. (44) at the order $O(\alpha)$ is obtained by solving $L_0\eta_1 = 0$ and is in the form $\eta_1 = \Gamma \exp[i(kx - \omega_r t)] + c.c$ where $\Gamma(x_1, t_1, t_2)$ is the nonlinear amplitude function and $c.c$ is its complex conjugate. The solution of the equation $L_0\eta_2 + L_1\eta_1 = -N_1$ at the $O(\alpha^2)$ is in the form $\eta_2 = \Omega\Gamma^2 \exp[2i(kx - \omega_r t)] + c.c$ Using the solutions for η_1 and η_2 in the $O(\alpha^3)$ equation given by $L_0\eta_3 + L_1\eta_2 + L_2\eta_1 = -N_3$, the equation for the perturbation amplitude $\Gamma(x_1, t_1, t_2)$ is obtained as

$$\frac{\partial\Gamma}{\partial t_2} + J_1\frac{\partial^2\Gamma}{\partial {x_1}^2} - \omega_i'\Gamma + (J_2 + iJ_4)|\Gamma|^2\Gamma = 0, \tag{45}$$

where

$$\omega_i' = \alpha^{-2}\omega_i, \tag{46a}$$

$$J_1 = B_1 - 6C_1k^2, \tag{46b}$$

$$\begin{aligned}J_2 = -A_1'H_{1i}k + \left(P_1'' - 5B_1'k^2 + 17C_1'k^4 + 4D_1k^2 - 10E_1k^4\right)H_{1r}\\ + \left(\frac{P_1'''}{2} - \frac{3}{2}B_1''k^2 + \frac{3}{2}C_1''k^4 + D_1'k^2 - E_1'k^4\right),\end{aligned} \tag{46c}$$

$$J_4 = \frac{1}{2}A_1''k + A_1'kH_{1r} + \left(P_1'' - 5B_1'k^2 + 17C_1'k^4 + 4D_1k^2 - 10E_1k^4\right)H_{1i}, \tag{46d}$$

where

$$Q_1 = -\frac{1}{2}P_1'' - ikA_1' + k^2(B_1' - C_1'k^2 + D_1 - E_1k^2), \tag{47a}$$

$$H_1 = H_{1r} + iH_{1i} = \frac{Q_1}{4k^2(4C_1k^2 - B_1) + P_1'}. \tag{47b}$$

The expressions of L_0, L_1, L_2, N_2, and N_3 are given in Appendix B.

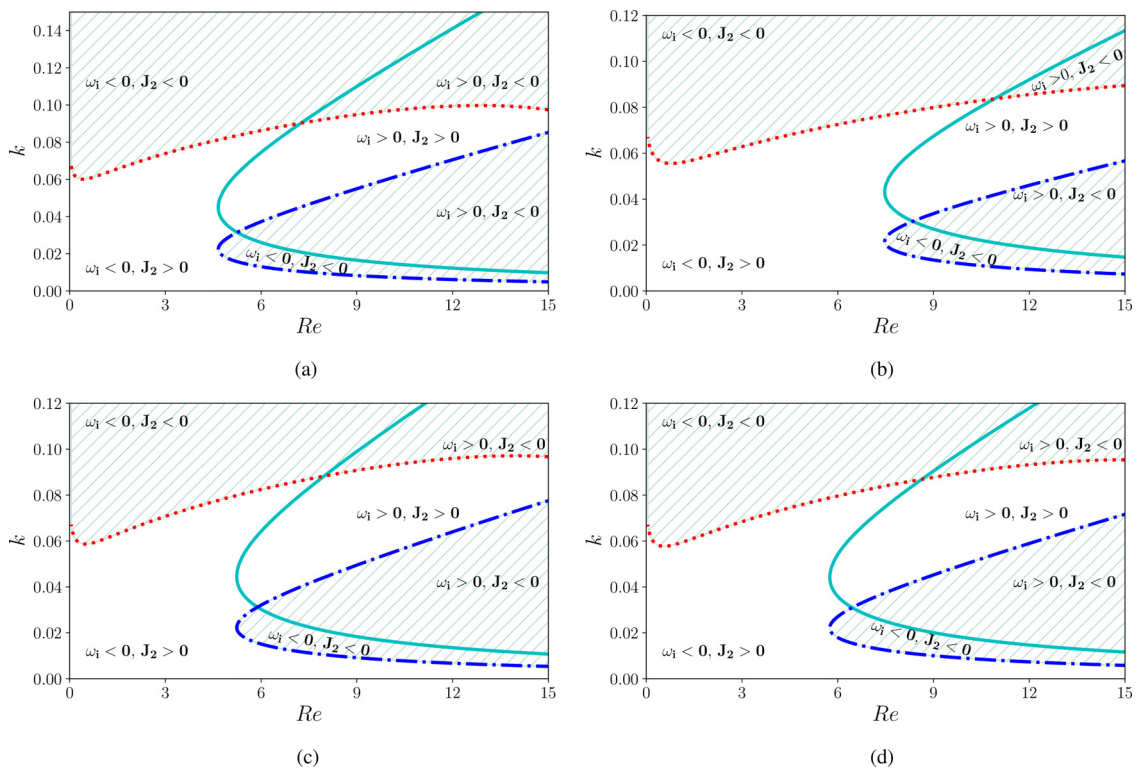

FIG. 6. Neutral stability curves for condensate film for (a) $\zeta = 0.1\pi$, downhill, (b) $\zeta = 0.1\pi$, uphill, (c) $\zeta = 0.02\pi$, downhill, and (d) $\zeta = 0.02\pi$, uphill. Curves are plotted for $Pr = 2.62$ and $Ka = 14\,133$, $Ku = 0.0872$, and for various values of bottom steepness ζ in downhill ($\hat{x} = 1.57$) and uphill ($\hat{x} = 4.71$). (a) $\zeta = 0.1\pi$, downhill; (b) $\zeta = 0.1\pi$, uphill; (c) $\zeta = 0.02\pi$, downhill; and (d) $\zeta = 0.02\pi$, uphill.

For detailed derivation of Eq. (45), we refer the reader to the studies by Mukhopadhyay and Haldar,[58] Mukhopadhyay and Mukhopadhyay,[48,52] Mukhopadhyay and Dandapat,[59] and the cross-reference therein.

The weakly nonlinear behavior of the flow can be investigated from Eq. (45). To solve Eq. (45), we assumed that the pertinent wave is filtered, giving us the freedom to eliminate the diffusion terms as there is no spatial modulation. With this assumption, the solution of (45) looks like

$$\Gamma = \Gamma_0(t_2)\exp\left[-i\,b(t_2)t_2\right]. \tag{48}$$

Substituting (48) in Eq. (45), we get

$$\frac{\partial \Gamma_0}{\partial t_2} = \left(\alpha^{-2}\omega_i - J_2\Gamma_0^2\right)\Gamma_0 \tag{49}$$

and

$$\frac{\partial (b(t_2)t_2)}{\partial t_2} = J_4\Gamma_0^2. \tag{50}$$

The term $(J_2\Gamma_0^2)\Gamma_0$, which is responsible for the acceleration or deceleration of the exponential growth of linear disturbance, appears on the right-hand side of Eq. (49) due to the nonlinearity.

The threshold amplitude of the disturbance is given by

$$\alpha\Gamma_0 = \left[\frac{\omega_i}{J_2}\right]^{\frac{1}{2}}, \tag{51}$$

and the nonlinear wave speed can be found as

$$Nc_r = c_r + c_i\frac{J_4}{J_2}. \tag{52}$$

Contrary to the linear wave speed (which is non-dispersive) discussed in the earlier in Sec. V A, Eq. (40), the nonlinear wave speed given in Eq. (52) is dispersive.

The term J_2 makes a major contribution in the study of weakly nonlinear analysis. For $J_2 = 0$, Eq. (49) is a linear differential equation of the filtered waves. The waves' amplitude grows and decays exponentially when $\omega_i < 0$ or $\omega_i > 0$. For $J_2 \neq 0$, its sign determines the ultimate nonlinear behavior of the system. When $J_2 > 0$, the bifurcation is supercritical and when $J_2 < 0$, it is subcritical.

Depending on the sign of J_2 and ω_i, different instability regions can be found as follows:

- Unconditional stable region: Here, $\omega_i < 0$ and $J_2 > 0$. In this region, finite amplitude disturbances are unconditionally stable.
- Subcritical unstable region: Here, $\omega_i < 0$ and $J_2 < 0$. In the linear stable region, finite amplitude disturbance can create instability.

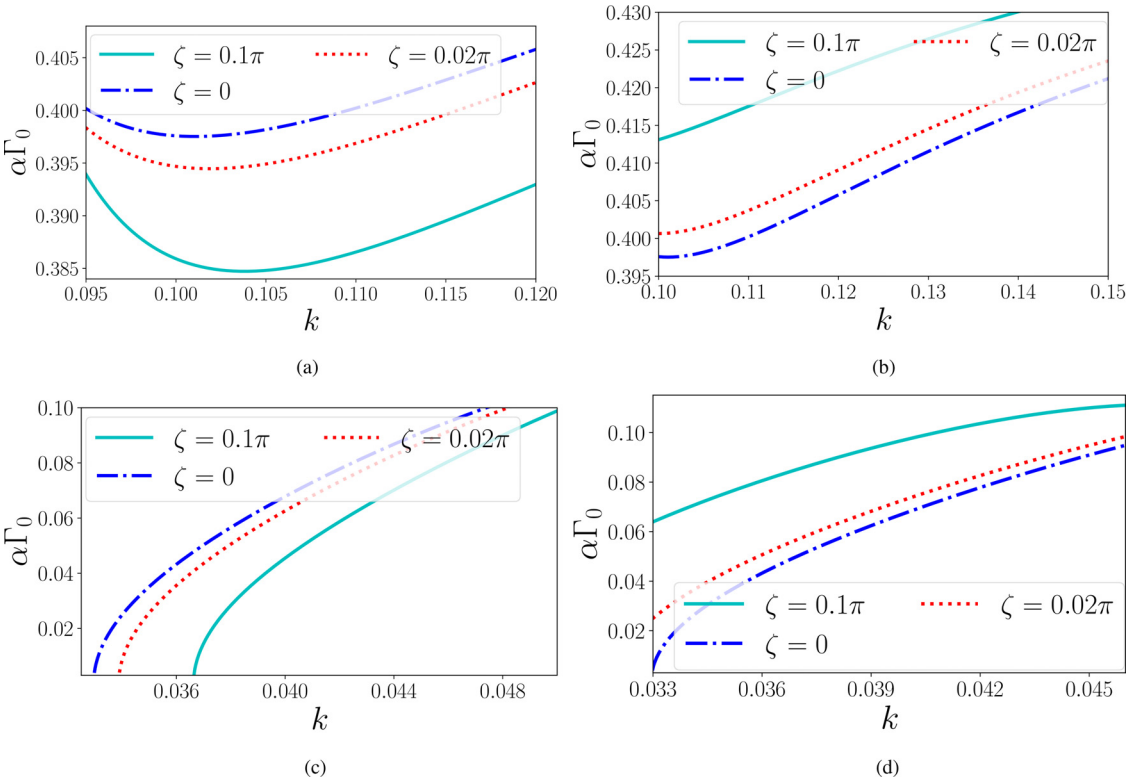

FIG. 7. Threshold amplitude for evaporating film for (a) downhill, subcritical; (b) uphill, subcritical; (c) downhill, supercritical; and (d) uphill, supercritical. Curves are plotted for $Pr = 2.62$ and $Ka = 14\,133$, $Ku = -0.0872$, and for various values of bottom steepness ζ in downhill ($\hat{x} = 1.57$) and uphill ($\hat{x} = 4.71$) and for $Re = 5$. (a) Downhill, subcritical; (b) uphill, subcritical; (c) downhill, supercritical; and (d) uphill, supercritical.

- Supercritical stable region: Here, $\omega_i > 0$ and $J_2 > 0$. In this linear unstable region, subsequent nonlinear growth of disturbance will configure a new equilibrium state with finite amplitude.
- Explosive region: Here, $\omega_i > 0$ and $J_2 < 0$. In this region, instability grows and makes the system unstable.

1. Results from the case study

Figure 5 reviles that, in the k–Re plane, only one subcritical region is found for evaporating films in contrast to the condensate film, where two distinct regions of subcritical instability are seen, one in the upper bound and the other in the lower bound of the linear stability region, which is shown in Fig. 6. Again, the unconditional stable region is much smaller for an evaporating film than a condensate film.

Also, it is clear that for flow in the uphill region, explosive zone decreases, and subcritical, supercritical, and unconditional stable zones increase significantly for both evaporating and condensate film, which confirms the stabilizing effect of the uphill region.

The weakly nonlinear stability analysis shows that the system will be unstable if the initial finite-amplitude disturbance is greater than the unstable threshold amplitude. Considering Figs. 7 and 8 that show the threshold amplitude for evaporating (for $Re = 5$) and condensate ($Re = 10$) film, respectively, in subcritical and supercritical regions, an interesting fact to be noticed here, in the downhill region, is that the increase in steepness decreases the threshold amplitude, i.e., giving a destabilizing effect. Conversely, in the uphill region, the opposite happens. Increasing the bottom steepness increases the threshold amplitude giving a stabilizing effect.

The wave speed predicted by the linear theory, given in (40), will not change for all wavenumbers, but the nonlinear wave speed, given by (52), can be influenced by the wavenumbers, but both of them are strongly dependent on Ku and other system parameters. The variations of the nonlinear wave speed with respect to wavenumber and different values of bottom steepness parameter ζ are shown in Fig. 9 (Fig. 10) for evaporating (condensing) film when $Re = 5$ ($Re = 10$). In the downhill region, increasing the bottom steepness increases the nonlinear wave speed, which confirms that bottom steepness gives a destabilizing effect. In contract to the uphill region, ζ gives a stabilizing effect by decreasing the nonlinear speed.

VI. NUMERICAL ANALYSIS

From governing equations and appropriate boundary conditions, we have derived the model (28), which is a single partial differential equation of the form

$$\frac{\partial h(x,t)}{\partial t} = f\left(h(x,t), \frac{\partial h(x,t)}{\partial x}, \frac{\partial^2 h(x,t)}{\partial x^2}, \frac{\partial^3 h(x,t)}{\partial x^3}, \ldots\right). \tag{53}$$

Using the method of line,[60] the spatial derivatives are approximated via the finite differences method, leading to a system of ordinary

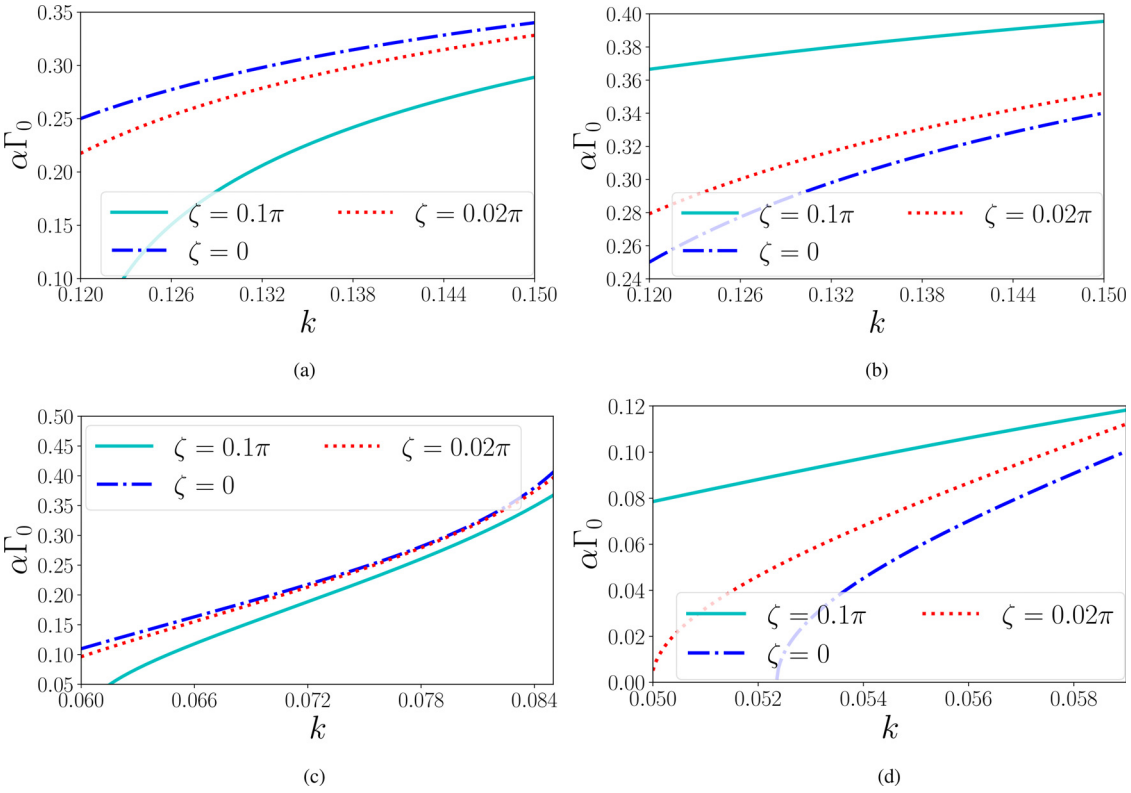

FIG. 8. Threshold amplitude for condensate film for (a) downhill, subcritical; (b) uphill, subcritical; (c) downhill, supercritical; and (d) uphill, supercritical. Curves are plotted for $Pr = 2.62$ and $Ka = 14\,133$, $Ku = 0.0872$ and for various values of bottom steepness ζ in downhill ($\hat{x} = 1.57$) and uphill ($\hat{x} = 4.71$) and for $Re = 10$. (a) Downhill, subcritical; (b) uphill, subcritical; (c) downhill, supercritical; and (d) uphill, supercritical.

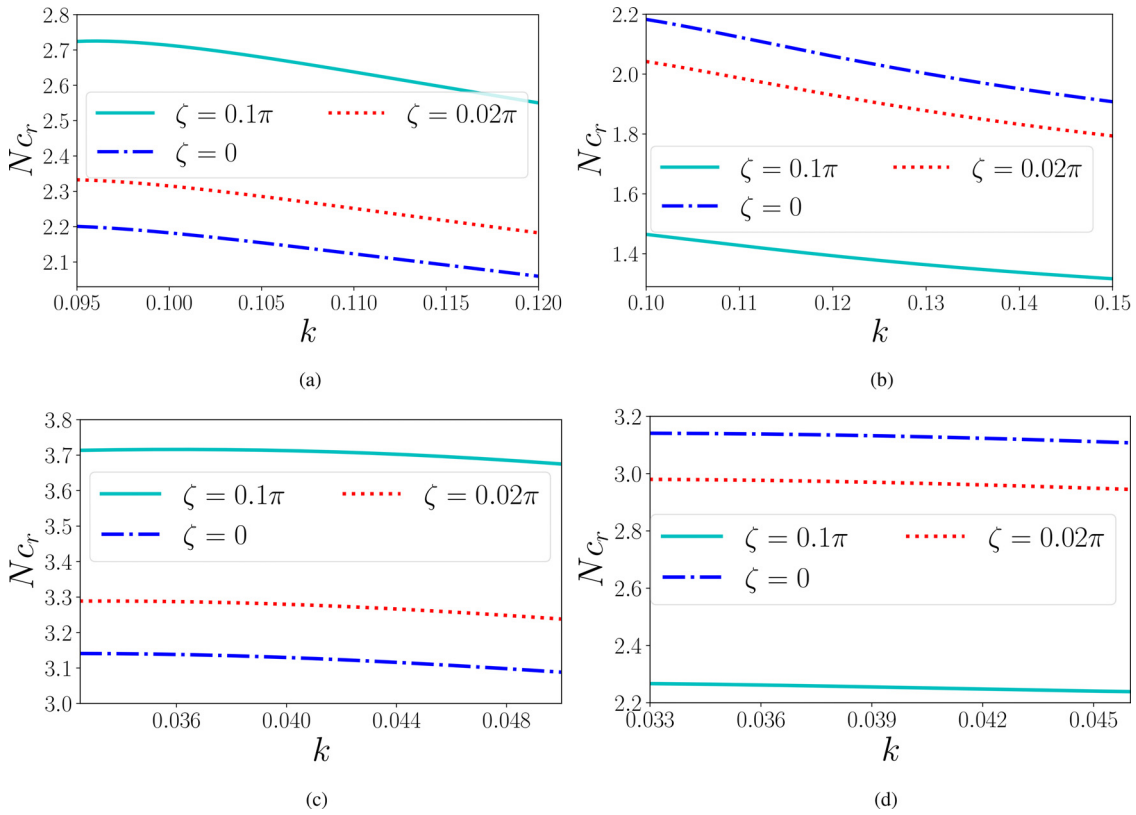

FIG. 9. Nonlinear wave speed for evaporating film for (a) downhill, subcritical; (b) uphill, subcritical; (c) downhill, supercritical; and (d) uphill, supercritical. Curves are plotted for $Pr = 2.62$ and $Ka = 14\,133$, $Ku = -0.0872$, and for various values of bottom steepness ζ in downhill ($\hat{x} = 1.57$) and uphill ($\hat{x} = 4.71$) and for $Re = 5$. (a) Downhill, subcritical; (b) uphill, subcritical; (c) downhill, supercritical; and (d) uphill, supercritical.

differential equations for the discrete h values on an even-spaced 1D grid. The local time evolution for h at the node i reads now as follows:

$$\frac{\partial h_i(t)}{\partial t} = \mathscr{F}(h_{i-2}(t), h_{i-1}(t), h_i(t), h_{i+1}, h_{i+2}(t)). \tag{54}$$

This dynamical system can then be solved using state-of-the-art ODE solvers. Initially, we impose a finite amplitude monochromatic disturbance as follows:

$$h(x, 0) = 1 + 0.1 \cos(2\pi x/L), \tag{55}$$

where $L = 2\pi/k$ is the length of the periodic domain and k is the wave number and solved Eq. (54) in periodic domain (i.e., assuming periodic boundary conditions).

As our one of the goals is to capture the rupture phenomena, it is essential to have a solver that will work with a small time step to be as close to the time where $\min(h(t)) \to 0$. We have chosen a 3/2 adaptive strong stability preserving (SSP) method with five stages (SSP coefficient 2, free second-order SSP interpolant).[61,62] This method is adaptive and comes with a (free) error estimation. This error estimation controls the time step during the simulation using a proportional-integral control algorithm (a PI controller). It also guarantees an error lower than some (relative or absolute) tolerance, rejecting any step that does not match these criteria. A relative tolerance reltol $= 10^{-6}$ has been chosen. The numerical scheme has been validated with previous works[48,51] and found to give consistent results.

As $\lim h \to 0$ lead to infinite values in the model, it is not possible to catch the exact moment where the film dry out: we use instead a linear extrapolation to obtain an approximation of t where $\min(h(x, t_{\text{rupt}})) = 0$, and the values for $h(x, t_{\text{rupt}})$. For the condensation case, the chosen Reynolds number is moderate ($Re = 10$). Due to the lack of free variable in the model, it is impossible to deal with long-running simulations with large fluid velocity. As injecting mass in the system leads to a thicker film with increased velocity, we have to end the simulation early. A simple root-finding algorithm is used to catch the moment where the h average reach a critical $\bar{h}(x) = 1.5$. A more complex model could be used in future work to overcome this limit.

A. Results from the case study

When $Ku < 0$, the mass loss due to evaporation is significant, and the film thickness changes with position and time $h = h(x, t)$. Figure 11 depicts the evolution of film interface as a function of time. It reveals that the growth of surface deformations becomes catastrophic when the wave trough approaches the point of rupture. The gradient of the film profile gradually increases as the film approaches toward rupture and jumps sharply to vary high values near rupture. This is because

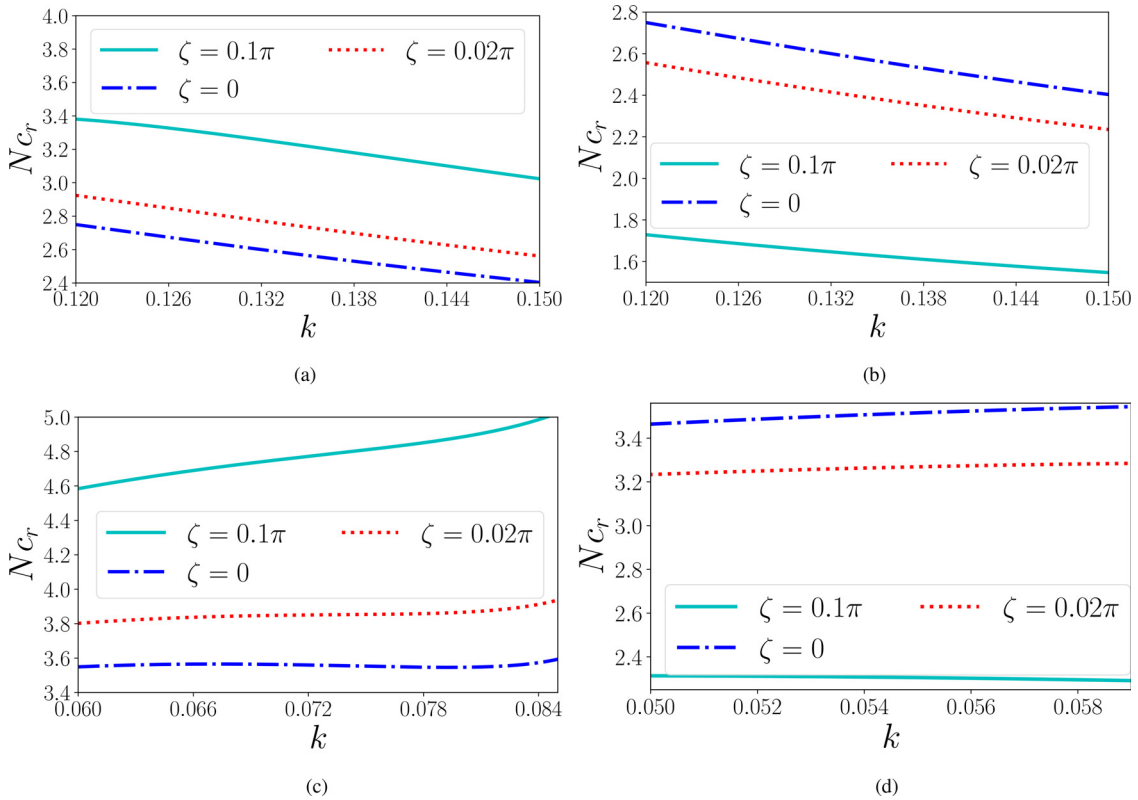

FIG. 10. Nonlinear wave speed for condensate film for (a) downhill, subcritical; (b) uphill, subcritical; (c) downhill, supercritical; and (d) uphill, supercritical. Curves are plotted for $Pr = 2.62$ and $Ka = 14\,133$, $Ku = 0.0872$, and for various values of bottom steepness ζ in downhill ($\hat{x} = 1.57$) and uphill ($\hat{x} = 4.71$) and for $Re = 10$. (a) Downhill, subcritical; (b) uphill, subcritical; (c) downhill, supercritical; and (d) uphill, supercritical.

the evolution of evaporating film is characterized by two simultaneous processes: the decrease in the average film thickness due to evaporation mass loss and the deformation of the initial flat liquid–vapor interface due to the flow of the film. The bottom steepness ζ does not have much impact on rupture time. Figure 11(d) shows the variation in rupture time for different Ku values. As Ku increases ($-Ku$ decreases), rupture time increases, i.e., giving a stabilizing effect.

Similarly, when $Ku > 0$, the mass gain due to condensation is significant. Figure 12 shows the evolution of film interface as a function of time for various Ku values and for different ζ. Here, the time to reach to $\bar{h}(x) = 1.5$ increases with decreasing Ku (for a fixed ζ), i.e., Ku is playing a destabilizing effect.

VII. CONCLUSION

Our main emphasis for the current work is to analyze the effect of bottom topography on the evolution of the film undergoing interfacial phase change (condensation/evaporation). The formulation of the problem is performed by transforming the governing equations and the pertinent boundary conditions in the curvilinear coordinate system. This transformation provides an easy but robust way to discuss such problems containing a curvy topography. The film evolution is governed by evaporation (condensation), mass loss (gain), and subsequent film thinning (thickening). The general assumptions in this study are that (1) Reynolds and Prandtl numbers are of order one; (2) slope of the interface is small (long waves); and (3) finally, the bottom steepness is moderate.[48,52] However, the maximum steepness is strongly restricted by the dependence of the surface on the local inclination angle $(\beta - \theta)$[27] for a given inclination angle β. After delicate investigation, we decided to choose the range of bottom steepness ζ from 0.0 to 0.4 when the inclination angle $\beta = \pi/3$ to make the model physically and geometrically consistent.

The classical long-wave expansion method is used to derive a surface evolution equation accounting for fluid's fundamental physical properties that are assumed as constant and the topographic nature of the bottom, and other essential characteristics like mean surface tension, gravity, etc., in terms of different non-dimensional number. Several assumptions have been adopted in the present study. The analysis of the phase change effect is not completely general. The temperature jump associated with the phase change[49] is not considered here. Generally, in the case of evaporation (condensation) in the liquid film, a steady uniform basic state is only permitted if it is time-dependent[23,49] but in our present study, this property is simplified by assuming the unperturbed film as steady and the perturbed equations to be unsteady locally. Our intention behind this is nothing but to simplify the entire analysis and to reduce the cost of computation so that the effect of bottom undulation can be easily understood for evaporating (condensate) film.

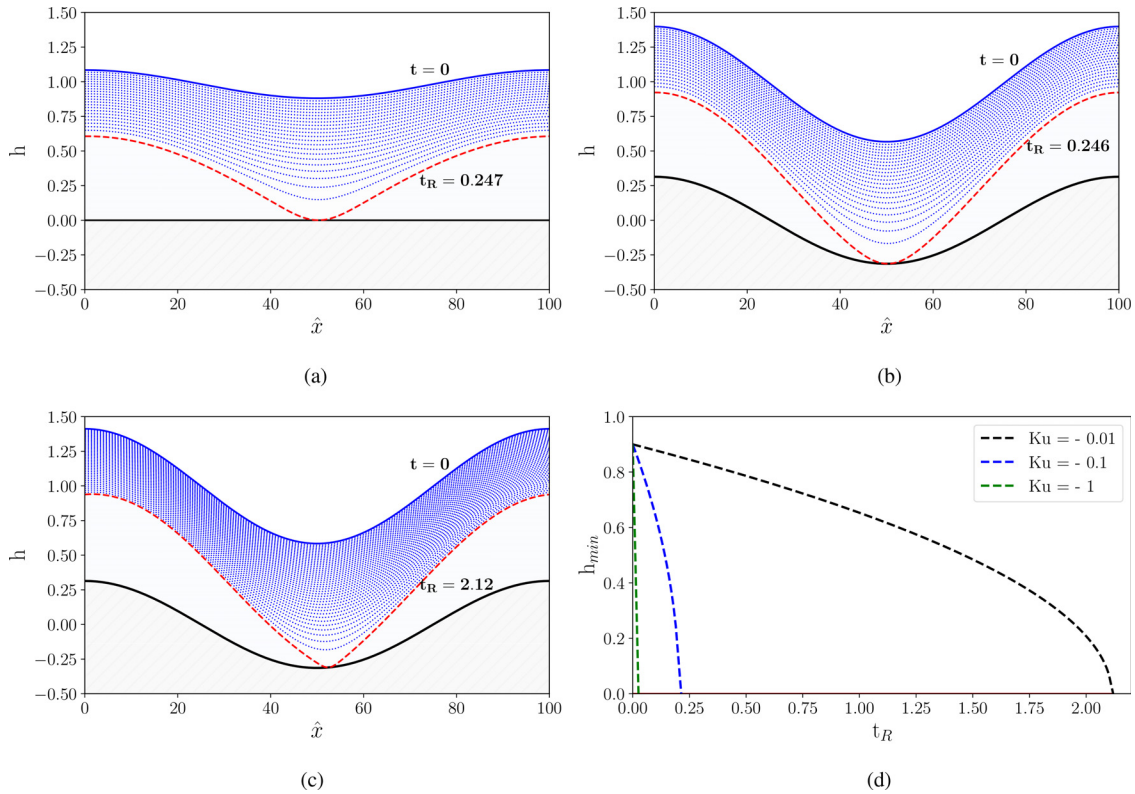

FIG. 11. Evaporating layers of films for various values of bottom steepness ζ and evaporation parameter Ku: (a) $\zeta = 0$, $Ku = -0.0872$, (b) $\zeta = 0.1\pi$, $Ku = -0.0872$, (c) $\zeta = 0.1\pi$, $Ku = -0.01$, and (d) $\zeta = 0.1\pi$. The curves are plotted for $Pr = 2.62$ and $We = 45\,000$, $Re = 2$. t_R indicates the rupture time. The period of the domain is taken as 100. (a) $\zeta = 0$, $Ku = -0.0872$; (b) $\zeta = 0.1\pi$, $Ku = -0.0872$; (c) $\zeta = 0.1\pi$, $Ku = -0.01$; and (d) $\zeta = 0.1\pi$.

The noticeable interesting results from the case studies are as follows:

- The bottom steepness ζ gives a dual effect on the uphill and downhill region for linear and weakly nonlinear analysis. This kind of behavior is claimed before in our earlier researches for Newtonian film flow with linear temperature variation[48] and for isothermal non-Newtonian flow[52] over the undulated bottom.
- In the downhill region, ζ destabilizes by decreasing the stable region area, and in the uphill region, it stabilizes by increasing the area of the stable region.
- ζ has no significant effect on the threshold of instability for an evaporating film but for condensate film, ζ shows the same dual effect on Re_c as mentioned above.

The weakly nonlinear waves have been investigated by using the method of multiple scales.

- The supercritical and subcritical solutions are possible for both evaporating and condensate film.
- Two distinct subcritical unstable zones are found for the condensate film, which brings a contrast to the evaporating film.
- The unconditional stable region is much smaller for an evaporating film than that of a condensate film.
- In the uphill region, unconditional stable zones are found to increase significantly for both evaporating and condensate films, which confirms the uphill region's stabilizing effect.
- The characteristics of the threshold amplitude and the nonlinear wave speed are discussed to be confirmed with the fact that ζ plays a dual role in the downhill and uphill region for both evaporating and condensate film.

The evolution of evaporating (condensing) film is characterized by two simultaneous processes: the decrease (increase) of average film thickness due to evaporation (condensation) mass loss (gain) and the deformation of the initial flat liquid–vapor interface due to the flow of the film. Studying the time-dependent evolution of the film's free surface, we can say the following:

- Film rupture happens for the evaporating film due to the mass loss. The dynamics highly depend on the initial perturbation because it ruptures before it can be developed into a stationary film.
- The bottom steepness ζ has no significant effect on rupture time, which can be explained as the bottom is heated uniformly. However, Ku gives a stabilizing effect.
- For condensate film, due to the gain of mass, film thickness increases rapidly.

Finally, the phase change effect for film flowing down a wavy inclined bottom has not been studied intensively so far. This paper significantly steps toward a new direction by identifying the effect of bottom steepness in phase change for a flowing film. Further improvements in

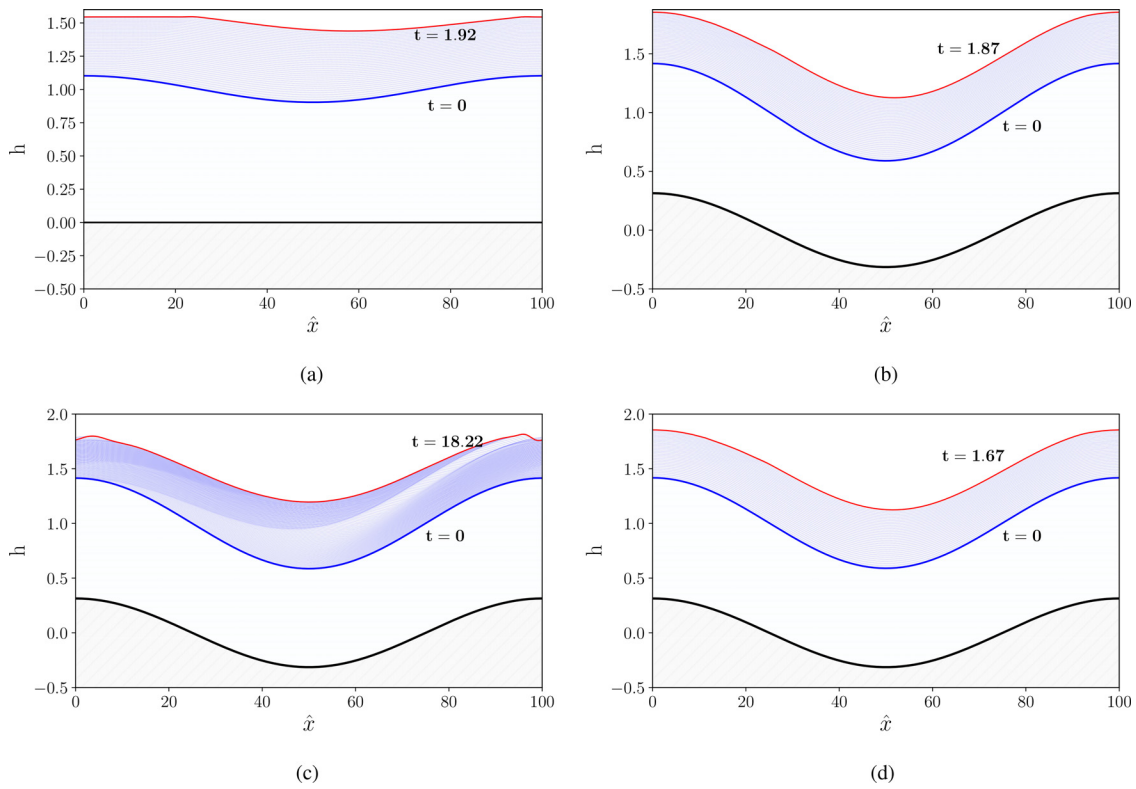

FIG. 12. Condensing layers of films for various values of bottom steepness ζ and condensation parameter Ku: (a) $\zeta = 0$, $Ku = 0.0872$, (b) $\zeta = 0.1\pi$, $Ku = 0.0872$, (c) $\zeta = 0.1\pi$, $Ku = 0.01$, and (d) $\zeta = 0.1\pi$, $Ku = 0.1$. The curves are plotted for $Pr = 2.62$ and $We = 45\,000$, $Re = 10$. t_R indicates the rupture time. The period of the domain is taken as 100. (a) $\zeta = 0$, $Ku = 0.0872$; (b) $\zeta = 0.1\pi$, $Ku = 0.0872$; (c) $\zeta = 0.1\pi$, $Ku = 0.01$; and (d) $\zeta = 0.1\pi$, $Ku = 0.1$.

modeling and numerics are required to understand the mechanism in more detail. We expect that our initiation will help for developing a rich understanding of this matter in the near future.

ACKNOWLEDGMENTS

The authors express their heartfelt gratitude to the anonymous referees for their attention to the manuscript and valuable comments and suggestions to improve the paper. The authors are delighted to express their optimum gratitude to the renowned scientist Professor Nuri Aksel for his valuable discussions and suggestions in this work. S.M. is thankful to Professor R. Usha, Professor Sanyasiraju V.S.S. Yedida, and the Department of Mathematics, IIT Madras, India, for giving the opportunity to work on the project CFD of Thin Film Flow on Substrates Featuring Topography.

AUTHOR DECLARATIONS

Conflict of Interest

The authors have no conflicts to disclose.

DATA AVAILABILITY

The data that support the findings of this study are available from the corresponding author upon reasonable request.

APPENDIX A: EQUATIONS AND SOLUTIONS OF LONG-WAVE EXPANSION MODEL

1. Zeroth-order equation

$$\frac{\partial u_0}{\partial x} + \frac{\partial v_0}{\partial y} = 0, \tag{A1}$$

$$3SS + \frac{\partial^2 u_0}{\partial y^2} = 0, \tag{A2}$$

$$-Re\frac{\partial p_0}{\partial y} - 3CS = 0, \tag{A3}$$

$$\frac{\partial^2 T_0}{\partial y^2} = 0. \tag{A4}$$

At $y = 0$

$$u_0 = 0, \quad v_0 = 0, \quad T_0 = 0. \tag{A5}$$

At $y = h$

$$\frac{\partial u_0}{\partial y} = 0, \tag{A6}$$

$$p_a - p_0 = \varepsilon^2 We(h_{xx} - \zeta\varepsilon^{-1}\kappa + 2\zeta^2\kappa^2 h), \tag{A7}$$

$$\frac{\partial h}{\partial t}=\frac{Ku}{\varepsilon Pe}\left(\frac{\partial T_0}{\partial y}\right)-u_0h_x-v_0, \tag{A8}$$

$$T_0=1. \tag{A9}$$

2. Zeroth-order solution

$$u_0=-3SS\left(\frac{1}{2}y^2-hy\right), \tag{A10}$$

$$\bar{u}_0=SSh^2, \tag{A11}$$

$$v_0=-3SSh_x\frac{y^2}{2}, \tag{A12}$$

$$p_0=p_a-\frac{3CS}{Re}(y-h)-\varepsilon^2We(h_{xx}-\zeta\varepsilon^{-1}\kappa+2\zeta^2\kappa^2h), \tag{A13}$$

$$T_0=\frac{y}{h}, \tag{A14}$$

$$h_t=-3SSh^2h_x+\frac{Ku}{\varepsilon Pe}\left(\frac{1}{h}\right). \tag{A15}$$

3. First-order equation

$$\frac{\partial u_1}{\partial x}+\frac{\partial v_1}{\partial y}+\zeta\kappa v_0+\zeta\kappa y\frac{\partial v_0}{\partial y}=0, \tag{A16}$$

$$Re\left(\frac{\partial u_0}{\partial t}+u_0\frac{\partial u_0}{\partial x}+v_0\frac{\partial u_0}{\partial y}\right)=-Re\frac{\partial p_0}{\partial x}+\zeta\kappa\frac{\partial u_0}{\partial y}+\frac{\partial^2u_1}{\partial y^2}, \tag{A17}$$

$$-Re\zeta\kappa{u_0}^2=-Re\frac{\partial p_1}{\partial y}+\frac{\partial^2v_0}{\partial y^2}, \tag{A18}$$

$$RePr\left(\frac{\partial T_0}{\partial t}+u_0\frac{\partial T_0}{\partial x}+v_0\frac{\partial T_0}{\partial y}\right)=\frac{\partial^2T_1}{\partial y^2}+\zeta\kappa\frac{\partial T_0}{\partial y}. \tag{A19}$$

At $y=0$

$$u_1=0,\quad v_1=0,\quad T_1=0. \tag{A20}$$

At $y=h$

$$\frac{\partial u_1}{\partial y}+\zeta\kappa\left(2h\frac{\partial u_0}{\partial y}-u_0\right)=0, \tag{A21}$$

$$p_1=\frac{2}{Re}\left(\frac{\partial v_0}{\partial y}+\frac{\partial u_0}{\partial y}h_x\right), \tag{A22}$$

$$T_1=0. \tag{A23}$$

4. First-order solution

$$\begin{aligned}u_1=&\frac{1}{2}ReSS\left(y^3-3yh^2\right)h_t\\&+ReSS\left[\frac{3}{8}SS\left(y^3-4h^3\right)hy\right]h_x+Re\left(\frac{y^2}{2}-hy\right)\\&\times\left[\frac{3CS}{Re}h_x-\varepsilon^2We\left(h_{xxx}-\zeta\varepsilon^{-1}\frac{\partial\kappa}{\partial x}+2\zeta^2\kappa^2h_x+4\zeta^2\kappa h\frac{\partial\kappa}{\partial x}\right)\right]\\&+\zeta\kappa\left[SS\left(\frac{1}{2}y^3-\frac{3}{2}hy^2+3h^2y\right)\right],\end{aligned} \tag{A24}$$

$$\begin{aligned}\bar{u}_1=&-\frac{5}{8}ReSSh^3h_t-\frac{27}{40}ReSS^2h^5h_x-\frac{1}{3}Reh\\&\times\left[\frac{3CS}{Re}h_x-\varepsilon^2We\left(h_{xxx}-\zeta\varepsilon^{-1}\frac{\partial\kappa}{\partial x}+2\zeta^2\kappa^2h_x+4\zeta^2\kappa h\frac{\partial\kappa}{\partial x}\right)\right]\\&+\frac{9}{8}\zeta\kappa SSh^3,\end{aligned} \tag{A25}$$

$$\begin{aligned}T_1=&\frac{\zeta\kappa}{2}\left(y-\frac{y^2}{h}\right)+Pe\left[\frac{3}{40}\frac{SSh_x}{h^2}y^5-\frac{3}{8}\frac{SSh_x}{h}y^4-\frac{1}{6}\frac{y^3}{h^2}h_t\right.\\&\left.+\frac{3}{10}SSh^2yh_x+\frac{1}{6}yh_t\right].\end{aligned} \tag{A26}$$

APPENDIX B: EXPRESSIONS

$$L_0\equiv\frac{\partial}{\partial t}+P_1'+A_1\frac{\partial}{\partial x}+B_1\frac{\partial^2}{\partial x^2}+C_1\frac{\partial^4}{\partial x^4}, \tag{B1a}$$

$$L_1\equiv\frac{\partial}{\partial t_1}+A_1\frac{\partial}{\partial x_1}+2B_1\frac{\partial^2}{\partial x\partial x_1}+4C_1\frac{\partial^4}{\partial x^3\partial x_1}, \tag{B1b}$$

$$L_2\equiv\frac{\partial}{\partial t_2}+B_1\frac{\partial^2}{\partial {x_1}^2}+6C_1\frac{\partial^4}{\partial x^2\partial {x_1}^2}, \tag{B1c}$$

$$\begin{aligned}N_2=&\frac{1}{2}P_1''\eta_1^2+A_1'\eta_1\eta_{1x}+B_1'\eta_1\eta_{1xx}+C_1'\eta_{1x}\eta_{1xxx}\\&+D_1\eta_{1x}^2+E_1\eta_1\eta_{1xxx},\end{aligned} \tag{B2}$$

$$\begin{aligned}N_3=&P_1''\eta_1\eta_2+A_1'\left[\eta_1(\eta_{2x}+\eta_{1x_1})+\eta_2\eta_{1x}\right]\\&+B_1'\left[\eta_1(\eta_{2xx}+2\eta_1\eta_{1xx_1})+\eta_2\eta_{1xx}\right]\\&+C_1'\left[\eta_1(\eta_{2xxxx}+4\eta_{1xxxx_1})+\eta_2\eta_{1xxxx}\right]\\&+D_1\left[2\eta_{1x}(\eta_{2x}+\eta_{1x_1})\right]+E_1\left[\eta_{1x}(\eta_{2xxx}+3\eta_{1xxx_1})\right.\\&\left.+\eta_{1xxx}(\eta_{2x}+\eta_{1x_1})\right]\\&+\frac{1}{2}A_1''\eta_1^2\eta_{1x}+\frac{1}{2}B_1''\eta_1^2\eta_{1xx}+\frac{1}{2}C_1''\eta_1^2\eta_{1xxxx}\\&+\frac{1}{6}P_1'''\eta_1^3+D_1'\eta_1^2\eta_{1x}+E_1'\eta_1\eta_{1x}\eta_{1xxx}.\end{aligned} \tag{B3}$$

REFERENCES

[1]P. Kapitza, "Wave flow of thin layers of viscous liquid. Part I. Free flow," Zh. Eksp. Teor. Fiz. **18**(1), 3–18 (1948).

[2]P. Kapitza and S. Kapitza, "Wave flow of thin layers of a viscous fluid: III. Experimental study of undulatory flow conditions," Zh. Eksp. Teor. Fiz. **19**(2), 105–120 (1949).

[3]T. B. Benjamin, "Wave formation in laminar flow down an inclined plane," J. Fluid Mech. **2**(6), 554–573 (1957).

[4]C.-S. Yih, "Stability of liquid flow down an inclined plane," Phys. Fluids **6**(3), 321 (1963).

[5]D. J. Benney, "Long waves on liquid films," J. Math. Phys. **45**, 150–155 (1966).

[6]M. Türkyilmazoğlu and A. I. Ruban, "The absolute instability of thin wakes in an incompressible/compressible fluid," Theor. Comput. Fluid Dyn. **13**(2), 91–114 (1999).

[7]M. Turkyilmazoglu, J. Cole, and J. Gajjar, "Absolute and convective instabilities in the compressible boundary layer on a rotating disk," Theor. Comput. Fluid Dyn. **14**, 21–37 (2000).

[8]S. P. Lin and C. Y. Wang, "Modelling wavy film flow," in *Encyclopedia of Fluid Mechanics: Vol. 1: Flow Phenomena and Measurement*, edited by N. P. Cheremisinoff (Gulf Publishing Company, Book Division, Houston, 1985), pp. 931–951.

[9]H. Chang, "Wave evolution on a falling film," Annu. Rev. Fluid Mech. **26**(1), 103–136 (1994).
[10]S. O'Brien and L. W. Schwartz, "Theory and modeling of thin film flows," in *Encyclopedia of Surface and Colloid Science*, Third Edition (2015), pp. 7377–7390.
[11]S. V. Alekseenko, V. E. Nakoriakov, B. G. Pokusaev, and T. Fukano, *Wave Flow of Liquid Films* (Begell House, New York/Wallingford, 1994).
[12]D.-Y. Hsieh and S. P. Ho, *Wave and Stability in Fluids* (World Scientific, 1994).
[13]H.-C. Chang and E. A. Demekhin, *Complex Wave Dynamics on Thin Films*, Studies in Interface Science, Vol. 14 (Elsevier, Amsterdam/New York, 2002).
[14]E. M. Sparrow, R. Eichhorn, and J. L. Gregg, "Combined forced and free convection in a boundary layer flow," Phys. Fluids **2**, 319–328 (1959).
[15]G. Bankoff, "Stability of liquid flow down a heated inclined plane," Int. J. Heat Mass Transfer **14**, 377–385 (1971).
[16]E. Marschall and C. Y. Lee, "Stability of condensate flow down a vertical wall," Int. J. Heat Mass Transfer **16**, 41–48 (1973).
[17]S. P. Lin, "Stability of liquid flow down a heated inclined plane," Int. J. Heat Mass Transfer **2**, 361–369 (1975).
[18]M. Ünsal and W. C. Thomas, "Linearized stability analysis of film condensation," J. Heat Transfer **100**, 629–634 (1978).
[19]M. Ünsal and W. C. Thomas, "Nonlinear stability of film condensation," J. Heat Transfer **102**, 483–488 (1980).
[20]B. Spindler, "Linear stability of liquid films with interfacial phase change," Int. J. Heat Mass Transfer **25**, 161–173 (1982).
[21]G. Kocamustafaogullari, "Two-fluid modeling in analyzing the interfacial stability of liquid film flows," Int. J. Multiphase Flow **11**, 63–89 (1985).
[22]C. C. Hwang and C. I. Weng, "Finite-amplitude stability analysis of liquid films down a vertical wall with and without interfacial phase change," Int. J. Multiphase Flow **13**, 803–814 (1987).
[23]S. W. Joo, S. H. Davis, and S. G. Bankoff, "Long-wave instabilities of heated falling films: Two-dimensional theory of uniform layers," J. Fluid Mech. **230**, 117–146 (1991).
[24]T. Gambaryan-Roisman, "Marangoni convection, evaporation and interface deformation in liquid films on heated substrates with non-uniform thermal conductivity," Int. J. Heat Mass Transfer **53**, 390–402 (2010).
[25]H. A. Abderrahmane, "Stability of an evaporating and condensing liquid film flowing down an inclined plane," Energy Procedia **142**, 3944–3949 (2017).
[26]C. Pozrikidis, "The flow of a liquid film along a periodic wall," J. Fluid Mech. **188**, 275–300 (1988).
[27]A. Wierschem, C. Lepski, and N. Aksel, "Effect of long undulated bottoms on thin gravity-driven films," Acta Mech. **179**, 41–66 (2005).
[28]Y. Y. Trifonov, "Stability and nonlinear wavy regimes in downward film flows on a corrugated surface," J. Appl. Mech. Tech. Phys. **48**, 91–100 (2007).
[29]Y. Y. Trifonov, "Stability of a viscous liquid film flowing down a periodic surface," Int. J. Multiphase Flow **33**, 1186–1204 (2007).
[30]H. Tougou, "Long waves on a film flow of a viscous fluid down an inclined uneven wall," J. Phys. Soc. Jpn. **44**, 1014–1019 (1978).
[31]E. Mogilevskiy and V. Shkadov, "Stability of a thin film flow on a weakly wavy wall," Int. J. Multiphase Flow **114**, 168–179 (2019).
[32]S. Veremieiev and D. H. Wacks, "Modelling gravity-driven film flow on inclined corrugated substrate using a high fidelity weighted residual integral boundary-layer method," Phys. Fluids **31**, 022101 (2019).
[33]C. Ruyer-Quil and P. Manneville, "Improved modeling of flows down inclined planes," Eur. Phys. J. B **15**, 357–369 (2000).
[34]S. J. D. D'Alessio, J. P. Pascal, and H. A. Jasmine, "Instability in gravity-driven flow over uneven surfaces," Phys. Fluids **21**, 062105 (2009).
[35]Y. Trifonov, "Nonlinear waves on a liquid film falling down an inclined corrugated surface," Phys. Fluids **29**, 054104 (2017).
[36]M. Vlachogiannis and V. Bontozoglou, "Experiments on laminar film flow along a periodic wall," J. Fluid Mech. **457**, 133–156 (2002).
[37]A. Wierschem and N. Aksel, "Instability of a liquid film flowing down an inclined wavy plane," Phys. D **186**, 221–237 (2003).
[38]A. Wierschem, M. Scholle, and N. Aksel, "Vortices in film flow over strongly undulated bottom profiles at low Reynolds numbers," Phys. Fluids **15**, 426–435 (2003).
[39]A. Wierschem, V. Bontozoglou, C. Heining, H. Uecker, and N. Aksel, "Linear resonance in viscous films on inclined wavy planes," Int. J. Multiphase Flow **34**, 580–589 (2008).
[40]L. A. Dávalos-Orozco, "Nonlinear instability of a thin film flowing down a smoothly deformed surface," Phys. Fluids **19**, 074103 (2007).
[41]L. A. Dávalos-Orozco, "Instabilities of thin films flowing down flat and smoothly deformed walls," Microgravity Sci. Technol. **20**, 225–229 (2008).
[42]T. Häcker and H. Uecker, "An integral boundary layer equation for film flow over inclined wavy bottoms," Phys. Fluids **21**, 092105 (2009).
[43]C. Heining and N. Aksel, "Bottom reconstruction in thin-film flow over topography: Steady solution and linear stability," Phys. Fluids **21**, 083605 (2009).
[44]C. Heining and N. Aksel, "Effects of inertia and surface tension on a power-law fluid flowing down a wavy incline," Int. J. Multiphase Flow **36**, 847–857 (2010).
[45]C. Heining, V. Bontozoglou, N. Aksel, and A. Wierschem, "Nonlinear resonance in viscous films on inclined wavy planes," Int. J. Multiphase Flow **35**, 78–90 (2009).
[46]N. Aksel and M. Schörner, "Films over topography: From creeping flow to linear stability, theory, and experiments, a review," Acta Mech. **229**, 1453–1482 (2018).
[47]A. Oron, S. H. Davis, and S. G. Bankoff, "Long-scale evolution of thin liquid films," Rev. Mod. Phys. **69**, 931–980 (1997).
[48]S. Mukhopadhyay and A. Mukhopadhyay, "Hydrodynamics and instabilities of falling liquid film over a non-uniformly heated inclined wavy bottom," Phys. Fluids **32**, 074103 (2020).
[49]J. P. Burelbach, S. G. Bankoff, and S. H. Davis, "Nonlinear stability of evaporating/condensing liquid films," J. Fluid Mech. **195**, 463–494 (1988).
[50]M. Ünsal and W. C. Thomas, "Perturbation solutions for laminar film condensation on nonisothermal walls," J. Appl. Mech. **43**, 367–368 (1976).
[51]S. Mukhopadhyay and A. Mukhopadhyay, "Interfacial phase change effect on a viscous falling film having odd viscosity down an inclined plane," Int. J. Multiphase Flow **143**, 103728 (2021).
[52]S. Mukhopadhyay and A. Mukhopadhyay, "Waves and instabilities of viscoelastic fluid film flowing down an inclined wavy bottom," Phys. Rev. E **102**, 023117 (2020).
[53]B. Uma and R. Usha, "Interfacial phase change effects on the stability characteristics of thin viscoelastic liquid film down a vertical wall," Int. J. Eng. Sci. **42**, 1381–1406 (2004).
[54]M. A. Ali, A. T. Jameel, and F.-R. Ahmadun, "Stability and rupture of nanoliquid film (NLF) flowing down an inclined plane," Comput. Chem. Eng. **29**, 2144–2154 (2005).
[55]E. J. Doedel, A. R. Champneys, T. F. Fairgrieve, Y. A. Kuznetsov, B. Sandstede, and X. Wang, "AUTO 97: Continuation and bifurcation software for ordinary differential equations," Technical Report (Department of Computer Science, Montreal Concordia University, Montreal, Canada, 2008), available at ftp.cs.concordia.ca in the directory pub/doedel/auto.
[56]R. D. Russell and J. Christiansen, "Adaptive mesh selection strategies for solving boundary value problems," SIAM J. Numer. Anal. **15**(1), 59–80 (1978).
[57]S. P. Lin and M. V. G. Krishna, "Stability of a liquid film with respect to initially finite three-dimensional disturbances," Phys. Fluids **20**, 2005–2011 (1977).
[58]A. Mukhopadhyay and S. Haldar, "Long-wave instabilities of viscoelastic fluid film flowing down an inclined plane with linear temperature variation," Z. Naturforsch. A **65**, 618–632 (2010).
[59]A. Mukhopadhyay and B. S. Dandapat, "Nonlinear stability of conducting viscous film flowing down an inclined plane at moderate Reynolds number in the presence of a uniform normal electric field," J. Phys. D: Appl. Phys. **38**, 138–143 (2004).
[60]W. E. Schiesser, *The Numerical Method of Lines: Integration of Partial Differential Equations*, 1st ed. (Academic Press, San Diego, 1991).
[61]S. J. Ruuth and R. J. Spiteri, "High-order strong-stability-preserving Runge–Kutta methods with downwind-biased spatial discretizations," SIAM J. Numer. Anal. **42**(3), 974–996 (2004).
[62]D. I. Ketcheson, S. Gottlieb, and C. B. Macdonald, "Strong stability preserving two-step Runge–Kutta methods," SIAM J. Numer. Anal. **49**, 2618–2639 (2011).